Available online at www.sciencedirect.com
SCIENCE DIRECT®
International Journal of Mass Spectrometry 228 (2003) 1–33
International Journal of Mass Spectrometry
www.elsevier.com/locate/ijms

Review

Stable isotope ratio mass spectrometry in global climate change research

Prosenjit Ghosh, Willi A. Brand*

Isotopen- und Gaslabor, Max-Planck-Institut für Biogeochemie, Postfach 100164, Jena 07701, Germany

Received 29 January 2003; accepted 20 May 2003

Abstract

Stable isotope ratios of the life science elements carbon, hydrogen, oxygen and nitrogen vary slightly, but significantly in major compartments of the earth. Owing mainly to antropogenic activities including land use change and fossil fuel burning, the $^{13}C/^{12}C$ ratio of CO_2 in the atmosphere has changed over the last 200 years by 1.5 parts per thousand (from about 0.0111073 to 0.0110906). In between interglacial warm periods and glacial maxima, the $^{18}O/^{16}O$ ratio of precipitation in Greenland has changed by as much as 5 parts per thousand (0.001935–0.001925). While seeming small, such changes are detectable reliably with specialised mass spectrometric techniques. The small changes reflect natural fractionation processes that have left their signature in natural archives. These enable us to investigate the climate of past times in order to understand how the Earth's climatic system works and how it can react to external forcing. In addition, studying contemporary isotopic change of natural compartments can help to identify sources and sinks for atmospheric trace gases provided the respective isotopic signatures are large enough for measurement and have not been obscured by unknown processes. This information is vital within the framework of the Kyoto process for controlling CO_2 emissions.

Keywords: Climate change; Stable isotopes; Carbon cycle; Isotope ratio mass spectrometry

1. Introduction

Man has followed and tried to understand climate for millenia, primarily driven by the need to assign the appropriate times for sowing and harvesting or to determine the timing for food and fuel storage necessary to survive during winter. Since our contemporary well-being still depends upon climate to some extent, there is a growing need to predict its future development at a range of temporal scales, its variability and associated potential hazards.

Owing to external forcing, the Earth's climatic system has always seen large variations [1–3]. Prediction of future climatic conditions will become possible provided we have a reasonably thorough understanding of the physico-chemical processes that are operating on the Earth's system. Detailed knowledge about the variability of physical and chemical processes driving

* Corresponding author. Tel.: +49-3641-576400; fax: +49-3641-5770.
E-mail address: wbrand@bgc-jena.mpg.de (W.A. Brand).

1387-3806/03/$ – see front matter © 2003 Elsevier B.V. All rights reserved.
doi:10.1016/S1387-3806(03)00289-6

the system may be obtained from natural archives (rocks, ice cores, sediments, etc.), which have been able to preserve a signature of major parameters like temperature, pH, pCO_2, etc.

Over the last decades, our ability to reconstruct past climate has considerably improved owing to the development of new sampling and measurement technologies. Key ingredients to this progress include high precision determination of trace gas concentrations and stable isotope ratios in samples of air, water, rocks and soils using chromatographic and mass spectrometric techniques. The objectives of studying isotopes in relation to past climate can be considered as a three tiered structure:

- to enable reconstruction of the range of natural climatic variability observed over the history of the earth. Of special interest are abrupt changes (i.e., occurring on a time scale comparable to a human life span) in periods not covered by contemporary observations;
- to test climate models using past environmental conditions in order to understand better how the present climate system works;
- by improved model calibrations, to enable predictions of future climate to be made with more confidence.

1.1. Role of isotopes; understanding the global carbon cycle

Atmospheric CO_2 provides a link between biological, physical and anthropogenic processes in ecosystems. Carbon and oxygen are exchanged between the atmosphere, the oceans, the terrestrial biosphere and, more slowly, with sediments and sedimentary rocks. Present concern is focused mainly on carbon because of its anthropogenic contribution, which includes fossil fuel combustion, deforestation, agriculture and cement production [4]. Each year approximately 120 Gt carbon are exchanged between the atmosphere and terrestrial ecosystems, and another 90 Gt between the atmosphere and the oceans [5]. In contrast, current annual fossil fuel burning amounts to about 6 Gt of carbon. About half of this amount is observed as an increase of the atmospheric CO_2 concentration. The other half is sequestered by other compartments. Currently, both the oceans and the terrestrial system show a net uptake of carbon [6]. The oxygen and carbon isotopic compositions of individual components, in particular air-CO_2 provide a potentially powerful tool towards quantifying the contribution of different components to ecosystem exchange. When this is used in conjunction with concentration or flux measurements, further insight can be gained into the sources and sinks of CO_2 in the ecosystem [7,8].

Plant photosynthesis discriminates against ^{13}C. In other words, plant carbon tends to have less ^{13}C than the CO_2 from which it is formed (Fig. 1). This discrimination provides a tool for interpreting changes in $\delta^{13}C$[1] of atmospheric CO_2 which can generally be applied in one of three ways:

- First, it can be used to partition net CO_2 fluxes between the land and the oceans. The known carbon budget for the last two decades is not closed fully, hence isotope measurements can help to locate the carbon sink missing so far as well as the processes involved in creating it. The missing carbon sink has been postulated from budget considerations to occur in the northern hemisphere [12]. This can be done because there is little carbon isotope discrimination associated with exchange of CO_2 between the ocean and atmosphere. Consequently, if the sink is in the land, changes in atmospheric CO_2 concentrations will be accompanied by changes in $\delta^{13}C$, whereas if the sink is due to absorption of CO_2 by

[1] The carbon isotopic composition is expressed as $\delta^{13}C$ which is defined as: $\delta^{13}C = \{[(^{13}C/^{12}C)_{sample} - (^{13}C/^{12}C)_{VPDB}]/(^{13}C/^{12}C)_{VPDB}\} \times 1000$. The standard defining the $^{13}C/^{12}C$ isotope scale is VPDB (Vienna Pee Dee Belemnite). The isotopic composition of CO_2 gas evolved from the original PDB (carbonate) by reaction with phosphoric acid under specific conditions has been determined by Craig [9]; by convention this gas is referred to as PDB-CO_2 [10]. The original PDB material no longer exists, and its further use as an isotopic reference is discouraged [11]. The VPDB scale has been introduced as a replacement [11]; it is accessed via NBS-19, a carbonate material whose composition is defined to be $\delta^{13}C = +1.95‰$ and $\delta^{18}O = -2.2‰$ relative to VPDB.

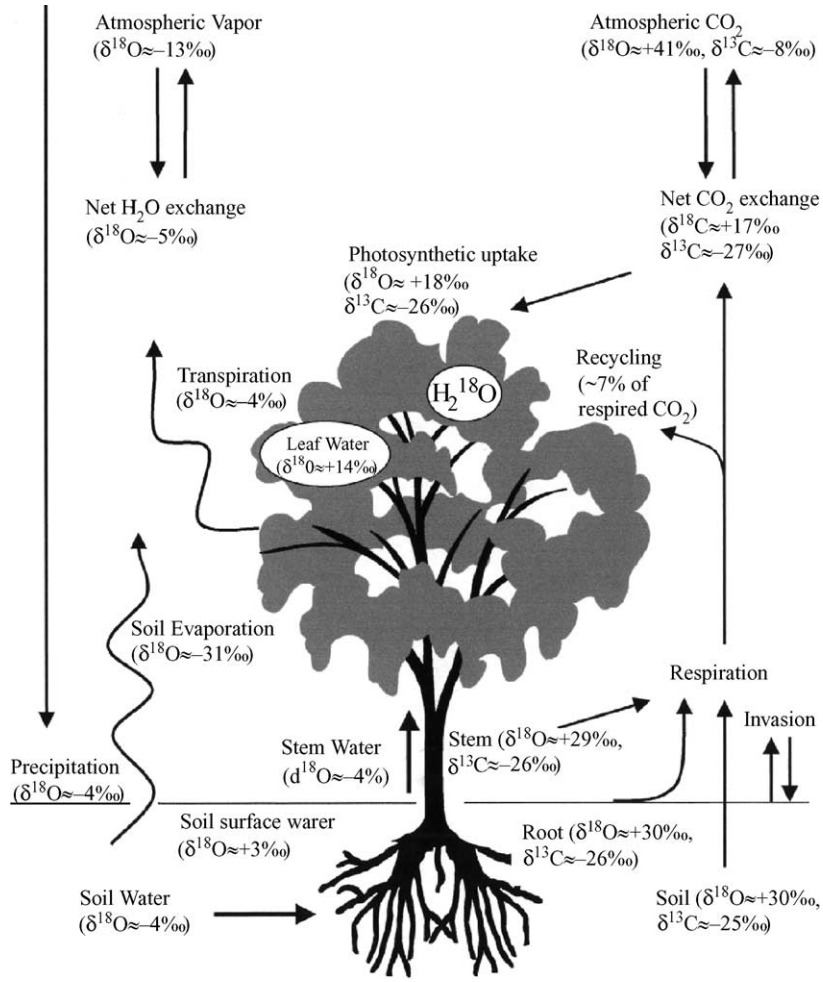

Fig. 1. Isotopic composition of C, O and H pools in terrestrial ecosystems. The values are approximations and will vary considerably with geographical location and environmental conditions. The actual data in the figure are from Israel (modified from Yakir and Sternberg [140]). $\delta^{18}O$ and δD values are given w.r.t. VSMOW and $\delta^{13}C$ values w.r.t. VPDB.

the ocean, changes in CO_2 concentrations will have little effect on $\delta^{13}C$.

- Second, on an ecosystem level discrimination by C_3[2] plants is influenced by environmental factors such as availability of light, water and nutrients, allowing to interpret changes in $\delta^{13}C$ of atmospheric CO_2 in terms of environmental changes, e.g., drought, El Nino and global warming [13].
- And third, since $\delta^{13}C$ of atmospheric CO_2 has changed over time, mainly due to addition of ^{13}C-depleted fossil fuel, carbon isotope ratios of respired (older) CO_2 differ slightly from those of (modern) photosynthesis. This isotope disequilibrium effect today renders the assessment of the relative contributions of respiration and photosynthesis to

[2] The two major pathways of photosynthesis are labelled C3 and C4, depending upon the number of carbon atoms comprising the first identifiable product of photosynthesis. The net discrimination across the C3 (Calvin) pathway is −16 to −18‰ relative to the atmospheric value whereas the overall C4 (Hatch-Slack) pathway effect is about −4‰. The majority of land plants follow the C3 pathway.

changes in atmospheric CO_2 difficult. On the other hand, with improved precision in local studies, it may help to unravel the respective signatures in the future.

The majority of land plants employ the C_3 (see footnote 2) photosynthetic pathway which results in a net ^{13}C depletion (~ -16 to $-18‰$) of the assimilated carbon with respect to the atmospheric value in CO_2 [14]. Around 21% of modern carbon uptake by plants occurs via C_4 (see footnote 2) photosynthesis, where the net discrimination against ^{13}C is smaller ($\sim -4‰$). As a result, the global mean carbon isotope discrimination is slightly smaller than the pure C_3 value, around $-15‰$ [15]. Release of CO_2 from fossil fuel involves combustion of coal and petroleum, most originally products of C_3 photosynthesis, and which have been additionally modified slightly over time by fractionation processes [16]. The isotopic composition of CO_2 released from fossil fuel combustion, biomass burning and soil respiration are generally similar. Hence, industrial and land use activities impose similar changes upon the $^{13}C/^{12}C$ ratio of the global atmosphere.

Most of the CO_2 in the air–sea system is dissolved in the oceans (>98%). Diffusion of CO_2 across the air–sea interface fractionates the $^{13}C/^{12}C$ ratio to about 1/10th the degree that does terrestrial photosynthesis [17]. The dissolved CO_2 in general is assumed to be in isotopic equilibrium with dissolved inorganic carbon (DIC) which contributes the bulk ($\sim$99%) of the mixed layer carbon. At the typical open ocean primary production rate [18], and considering time spans of centuries, marine photosynthesis *globally* has minimal impact on atmospheric CO_2 isotope values, mainly because any effect would be diluted by DIC within the mixed layer before reaching the atmosphere. As a consequence, atmospheric $^{13}C/^{12}C$ records can be used to partition the uptake of fossil fuel carbon between oceanic and terrestrial reservoirs [19]. They can also be used in studies of natural variability in the carbon cycle [20] and in calibrating global carbon budget models [21].

Fig. 1 summarises the influence of biospheric processes in individual compartments upon stable isotopes ratios of water and CO_2. Unlike carbon, the oxygen ratio ($^{18}O/^{16}O$) of atmospheric CO_2 is primarily determined by isotope exchange with leaf water, soil water and surface sea water [22,23]. During photosynthetic gas exchange oxygen atoms are transferred between carbon dioxide and leaf water within the cells' chloroplasts of a photosynthesizing leaf. This equilibrium exchange reaction occurs in the presence of the enzyme carbonic anhydrase, which acts as a potent catalyst for the readily reversible hydration/dehydration reaction [24]. The equilibrium of the exchange reaction in this case is reached so fast that it exceeds the CO_2 fixation by far and the CO_2 rediffusing back into the atmosphere carries the leaf water ^{18}O signal. The chloroplast water is usually enriched in ^{18}O relative to soil water owing to evaporation from the leaves where $H_2{}^{16}O$ evaporates preferentially relative to $H_2{}^{18}O$. This relative ^{18}O enrichment of chloroplast water (with respect to soil water) is sensitive to relative humidity and temperature, both of which are highly variable in different regions of the globe. Oxygen atom exchange with soil water occurs mainly through CO_2 from soil respiration, which slowly diffuses to the atmosphere. Oxygen atom exchange with sea water occurs through the exchange of CO_2 molecules across the air–sea interface. The net effect of ecosystem specific exchange reactions can be observed in the CO_2 of regional atmosphere samples when sampling is made with high spatial and temporal resolution [25].

The oxygen isotopic composition of soil and leaf water can vary considerably ($-25‰$ to $+25‰$ [26,27]). Soil water tends to follow the isotope composition of precipitation which is progressively depleted in $\delta^{18}O$ relative to sea water towards high latitudes and towards the interior of a continent. In contrast to phenomena occurring at higher latitudes, there is no correlation between surface temperature and $\delta^{18}O$ values of precipitation in the tropics [28]. Tropical regions are characterised by converging air masses that are forced to move vertically rather than horizontally. As a result they cool predominantly

by convection in atmospheric towers, while surface temperature gradients remain negligible. Although temperature does not correlate with $\delta^{18}O$ in the tropics, a negative correlation has been observed between the annual precipitation and $\delta^{18}O$ values at tropical island locations [28].

The isotopic composition of palaeo-water and paleo-atmosphere CO_2 can be obtained directly from ice core samples and trapped inclusions within ice cores. Indirectly, an estimation of the isotopic composition of past precipitation and atmosphere can also be made from analysis of proxy records like skeletal remains of animals, lake sediments and soil minerals that have formed in equilibrium with their surrounding environment.

In the following we review contemporary methods for determining stable isotopes relevant to climate research, in particular for trace gases in air, water and ice, and for plant and animal organic matter. Areas of global change research are discussed where isotope measurements have contributed significantly, including climate models and their relation to experimental observations.

2. Key experimental techniques for measuring stable isotope ratios relevant to climate research

2.1. Basic mass spectrometric designs for stable isotope ratio determination

Mass spectrometers for the measurement of stable isotope ratios are specialised magnetic sector, mostly single focusing instruments which can precisely determine relative intensities of the ion beams generated by a very limited number of gaseous compounds. Further mass spectrometric components include a high efficiency EI ion source, simultaneous ion current detection in an array of Faraday cups positioned along the image plane and an inlet system for handling the pure gases without isotopic fractionation, contamination, or memory (Fig. 2).

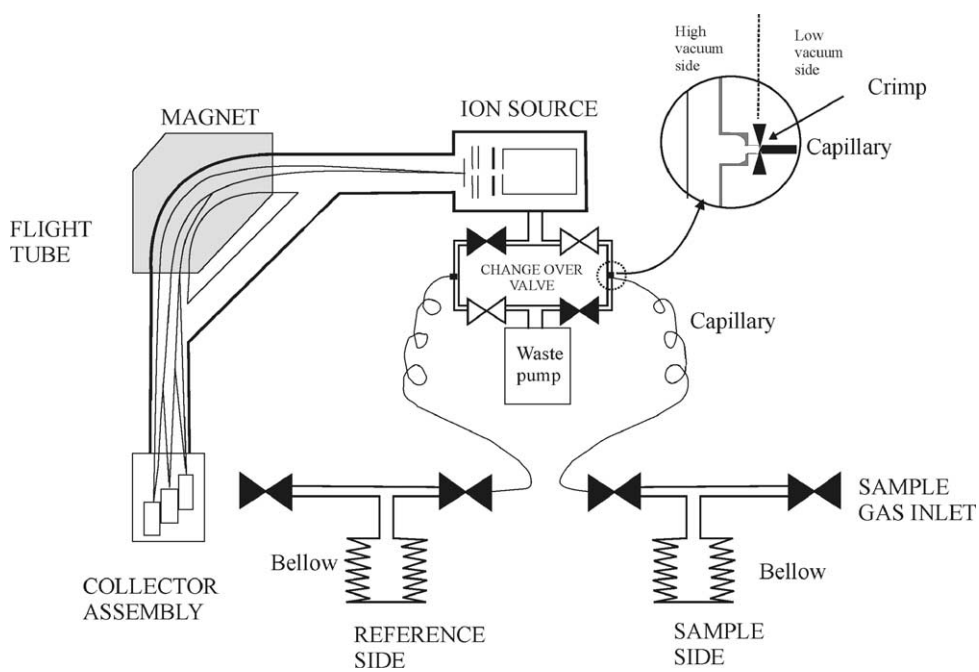

Fig. 2. Essential components of a gas isotope ratio mass spectrometer with Dual Inlet system. In the upper right a close up view of the capillary with crimp is shown for clarity.

The gases in question are mainly CO_2, N_2, H_2 and SO_2. All material where isotope ratios of C, N, O, H or S shall be determined, must be converted to one of these gases for measurement. Less frequently, other gases including O_2, N_2O, CO, SF_6 and CF_4 are used for isotopic analysis.

2.2. Inlet systems (classical Dual Inlet)

Inlet systems for gas isotope mass spectrometers comprise valves, pipes, capillaries, connectors and gauges. Home made inlets were often made of glass, but today commercial systems prevail which are mainly designed from stainless steel. The heart of the inlet system is the change-over-valve [29], which allows gases from the sample and the reference side to alternately flow into the mass spectrometer. The gases are fed from their reservoirs to the change-over-valve by capillaries of around 0.1 mm i.d. (internal diameter) and about 1 m in length with crimps for adjusting gas flows at their ends. Flow through both capillaries is constantly maintained, allowing one gas to enter the mass spectrometer while the other is directed to a vacuum waste pump. The smallest amount of sample that can be analysed using such a Dual Inlet system is limited by the requirement to maintain viscous flow conditions. As a rule of thumb, the mean free path of a gas molecule should not exceed 1/10th of the capillary dimensions. With the capillary dimension of 0.1 mm i.d., the lower pressure limit of viscous flow and thus accurate measurement is about 15–20 mbar. Due to this requirement it is necessary to concentrate the gas of interest into a small volume in front of the capillary when trying to reduce sample size. In conventional operation such volumes can be as low as 250 μL. For condensable gases, a small cold finger can be introduced between reservoir and mass spectrometer inlet. This arrangement enables to measure the isotopic composition from ∼500 nmol of sample gas.

The relative deviation in isotopic ratios between sample and standard is expressed in the δ notation with the δ-values commonly expressed in parts per thousand (per mill, ‰) (see footnote 1). Primary reference scales are maintained by the IAEA Isotope Hydrology Section [30] in Vienna. Carbon isotope ratios are referred to VPDB (Vienna Pee Dee Belemnite), oxygen values to VPDB or VSMOW (Vienna Standard Mean Ocean Water) [10,31]. Other reference scales include VCDT (for sulfur) and atmospheric N_2 (for nitrogen). VPDB is also a common reference scale for oxygen isotope ratios in the carbonate community and when isotope ratios of CO_2 in air are concerned. VSMOW also serves as origin of the international isotope scale for hydrogen isotopes.

2.3. Techniques for analysis of organic compounds

Organic compounds essentially comprise of carbon, nitrogen, hydrogen and oxygen. For isotopic measurements, CO_2, N_2 and H_2O are generated by oxidative combustion: $[C, H, N, O] + O_2 \Rightarrow CO_2 + H_2O + N_2$ (stoichiometry depends on the nature of the sample). Classically, the reaction is performed around 850 °C in sealed quartz or Pyrex tubes with CuO as the oxygen source. Following combustion, the sealed tubes are broken one by one on a vacuum line, the product gases are released and cryogenically separated and collected. While preparing samples for nitrogen analyses, CaO can be added to the quartz tube as a CO_2 absorber. Before analysis, H_2O is removed from the gas mixture. It can be used for *D*/*H* determination by conversion to H_2. Such hydrogen gas preparation requires a reducing agent like uranium at a temperature around 800 °C [32]. Alternative reduction reagents are Cr, Zn, Mn or pure C. For small samples, the product hydrogen gas can be collected on pure charcoal or can be compressed to the required inlet pressure using a Toepler pump.

More recently, interfacing isotope ratio mass spectrometry (IRMS) with gas chromatography (GC) has revolutionised compound specific isotope analyses (Fig. 3). In this technique, helium is used as a carrier and a reference gas is introduced into the carrier gas. A Dual Inlet system is not needed. Most progress has been made in measurement of ^{13}C abundances by combustion of GC separated compounds to CO_2 (plus other compounds) and the subsequent determination of: $^{12}C^{16}O^{16}O$:$^{13}C^{16}O^{16}O$ ratios [33,34]. The direct

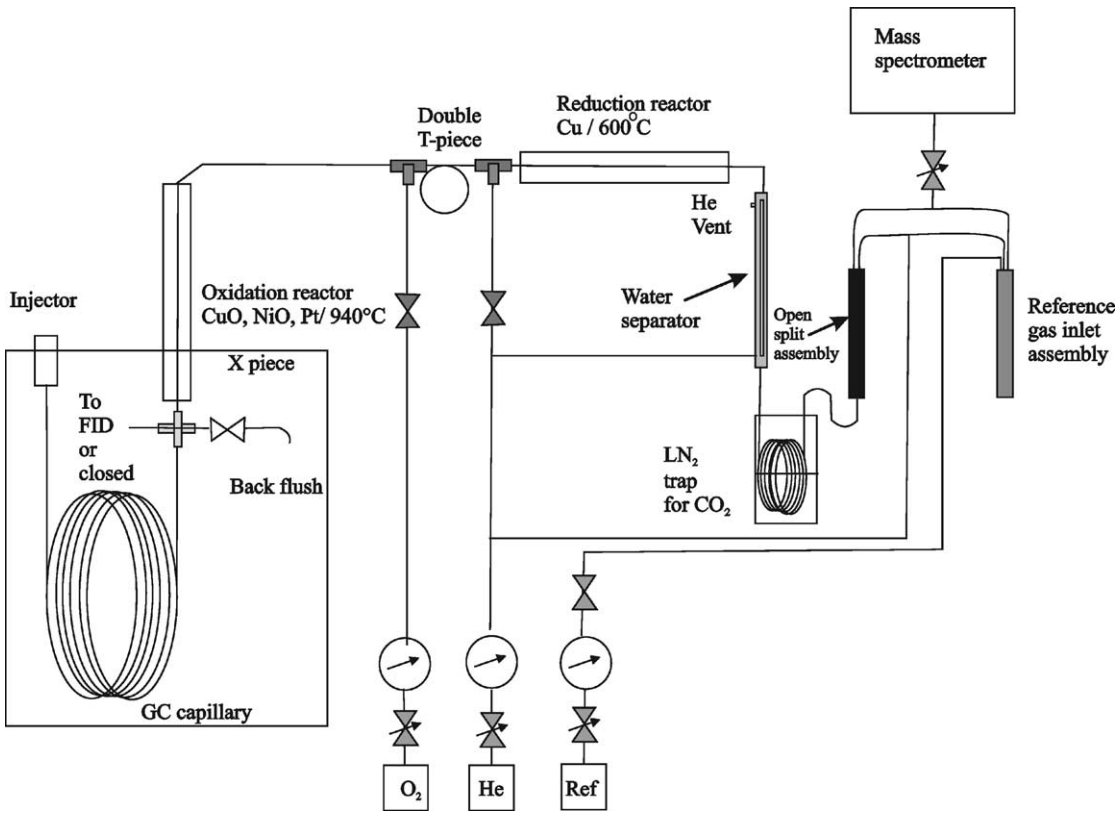

Fig. 3. Schematic diagram showing the basic setup for combustion of organic compounds eluting from a gas chromatograph (redrawn from Brand [46]).

measurement of $\delta^{18}O$ of organic compounds involves conversion of sample oxygen to a single gaseous product like CO. In order to quantitatively produce CO gas from organic material, a carbon reduction reaction at temperatures >1200 °C has proven valuable. Online pyrolysis IRMS techniques have been developed for $\delta^{18}O$ measurement in milligram quantities of cellulose, carbohydrates and aromatic compounds in the presence of glassy carbon at temperatures in excess of 1200 °C [35,36] and are increasingly utilised also for high precision work. After proper suppression of low energy helium ions in the mass spectrometer, the technique now allows to measure *D*/*H* ratios, too [37].

Online isotopic analysis is an area of rapid development at present. In climate research, it is being used for analysing trace gases like CH_4, CO, N_2O and also CO_2 (see examples further down).

2.4. Equilibration of water samples with CO_2, analysis of ice core samples

During evaporation and condensation processes the isotopic composition of water is altered. Gas phase water is lighter than the associated liquid phase. The degree of fractionation in this process depends upon temperature. Measurement of ice $\delta^{18}O$ and $\delta^{2}H$ obtained from Greenland and Antarctic ice cores can be taken as a proxy for the regional temperature at the time of snow/ice formation. It is a central measurement for the detection of past changes in climate (see further down).

The general method for the isotopic analysis of water samples is equilibration of the oxygen isotopes of gaseous CO_2 with those of the (liquid) water sample [38]. This is done under vacuum conditions at constant

temperature. Using this conventional method for paleoclimatological studies is, however, time consuming: the ice core has to be cut into small sections which are separately packed with preparation and measurement undertaken individually for each sample. A recently introduced technique [39] allows the measurement of $^{18}O/^{16}O$ ratios in a continuous flow fashion: A small block of sample ice is firmly positioned and held on a heated device, where the ice melts continuously. The melt water is then pumped off through a 1 cm × 1 cm bore hole in the centre of the melt head. After this, about 25% of the melt water is used for the actual measurement, the rest serving to seal the melted air water mixture from ambient air. The sample water is then loaded with CO_2 in a bubble generator and isotopic equilibration is achieved at 50 °C within a long capillary. Using helium as a carrier gas the equilibrated CO_2 (now carrying the ^{18}O signature of the water sample) is liberated in a degassing station consisting of a gas permeable membrane. The analyte is swept through a water trap before finally entering the IRMS via an open split for isotopic determination.

2.5. Isotope ratio measurements on CO_2 in air samples, key issues to ensure accuracy and precision

Global change issues have become significant due to the sustained rise in atmospheric trace gas concentrations (CO_2, N_2O, CH_4) over recent years, attributable to the increased per capita energy consumption of a growing global population. Since the isotopic signature of these trace gases can provide information about the origin and fate of the gases, the ability to measure their isotopic signature has become a useful tool in the study of the nature and distribution of sources and sinks of these trace gases. Experimental challenges to precisely measure isotopic ratios of these gases arise from factors like small ambient concentrations or small concentration differences as well as problems with the separation and isolation of the required species. In particular, gas separation and isolation techniques require considerable dedication. They are extremely time-consuming given the uncertainties arising from possible isotopic fractionation in each individual step of the preparation.

One of the first air CO_2 extraction systems was designed at CSIRO (Aspendale) in 1982 for routinely analysing air samples collected at Cape Grim (Tasmania) [40]. The Cape Grim in situ extraction line employs three high-efficiency glass U-tube traps with internal cooling coils. At Cape Grim, a vacuum pump draws air from either a 10 or 70 m high intake, and sampling alternates between the two intakes. Air from the intake is dried using a cold trap at about −70 °C. CO_2 is collected in a second trap immersed in liquid nitrogen. A third liquid nitrogen trap guards against oil vapour back-streaming from the vacuum pump. Air flow is maintained at 300 mL min^{-1} for 2 h, usually during late morning when the air masses are coming from the clean air sector. After this time, the temperature of the trap holding the CO_2 is raised to −70 °C, and the CO_2 is transferred cryogenically into a 100 mL glass flask for transport to CSIRO's Division of Atmospheric Research in Aspendale. Mass spectrometric analysis for $\delta^{13}C$ and $\delta^{18}O$ is carried out in Aspendale usually within one month after collection.

In addition, whole air samples are collected in 500 mL flasks. In this case, CO_2 ($+N_2O$) is cryogenically separated in an automated trapping line. The trapping setup (Fig. 4) is based on an automated trapping protocol described in Allison and Francey [41]. 20 to 40 mL of air is allowed to pass through assemblages of two cryotraps. All condensable material including CO_2 is collected initially in the first trap. CO_2 ($+N_2O$) is then slowly distilled into the second trap by raising the temperature of the first trap from −180 °C to about −100 °C. From the second trap the CO_2 is further transferred to a micro-volume cold finger. Including analysis with the mass spectrometer the whole process takes about 15 min per flask sample.

In 1989, the stable isotope laboratory at the Institute of Arctic and Alpine Research (INSTAAR, University of Colorado) started routine measurement of CO_2 isotopes from air samples collected at the network sites operated by NOAA-CMDL (Climate Monitoring and Diagnostics Laboratory). The mass spectrometers are fitted with manifold and extraction system. The

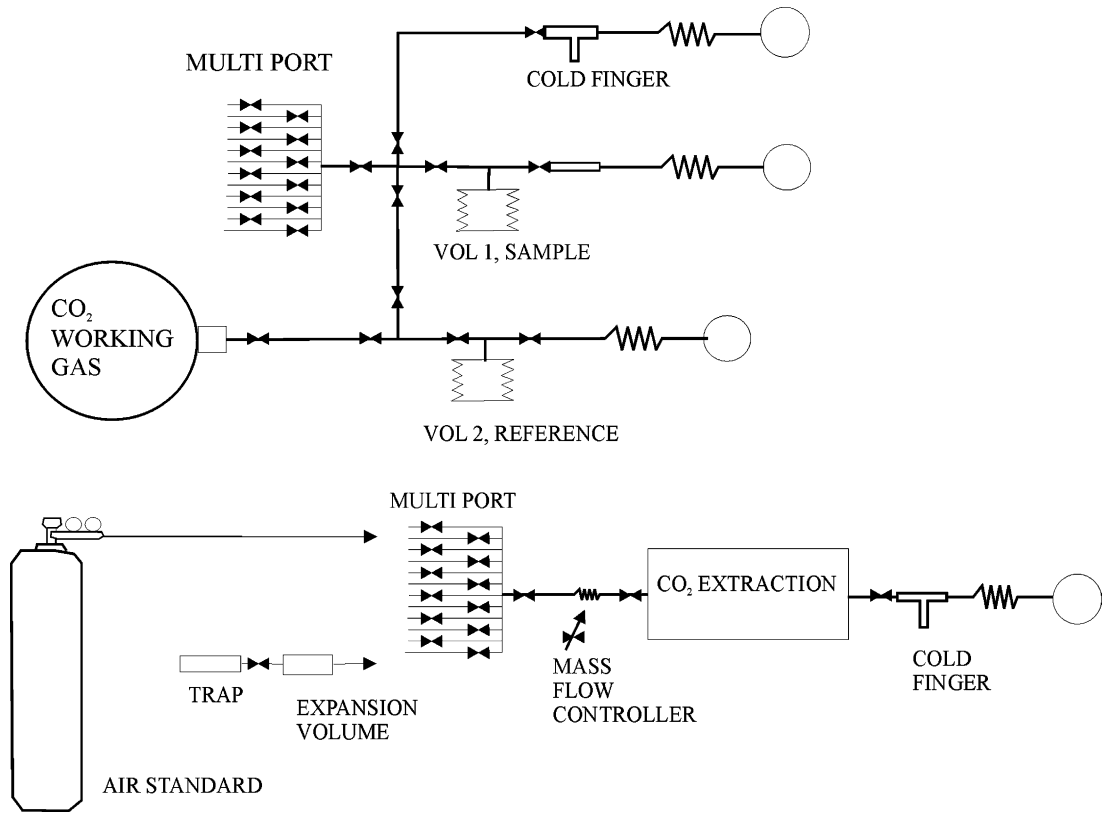

Fig. 4. Inlet system of the MAT 252 mass spectrometer and trapping box MT Box C (Finnigan MAT, Bremen), used for analyses of CO_2 from air and ice core samples at CSIRO, Aspendale (Melbourne) (redrawn from Allison and Francey [41]).

design of the extraction system differs slightly from the CSIRO unit (Fig. 5). The sample is diverted first through a dual loop glass trap (filled with glass beads) at −70 °C followed by a CO_2 trap at −196 °C. From here, the analyte gas is transferred to the sample inlet bellows for analysis with the mass spectrometer (further details may be found in ref. [42]).

In 1996, Trolier et al. [43] presented a 4-year time series of atmospheric CO_2 isotope measurement from several NOAA-CU sampling stations. Allison et al. [31] established a close agreement in $\delta^{13}C$ calibration between NOAA and CSIRO-DAR in Australia, which allowed for the merging of the two data sets for a two-dimensional modelling study [44]. As a conclusion, a strong terrestrial CO_2 sink operative in the northern mid-latitudes during 1992 and 1993 was postulated.

The initially small group of laboratories has grown steadily over the years. At the Max Planck Institute for Biogeochemistry (Jena), we have recently developed a new high precision air-CO_2 extraction line for automatic handling of air samples [45]. Like in the other laboratories, the air is sampled dry in order to maintain the $\delta^{18}O$ signature in the flasks during transport and storage. The device is coupled directly to a Finnigan MAT 252 isotope ratio mass spectrometer (IRMS). Table 1 gives a comparison of various parameters used in the extraction systems at NOAA-CMDL, CSIRO-DAR and MPI-BGC.

2.5.1. N_2O correction

Separating the relative ion current contributions of $CO_2^{\bullet+}$ and $N_2O^{\bullet+}$ in isotopic measurement is essential as both of them have nearly identical molecular

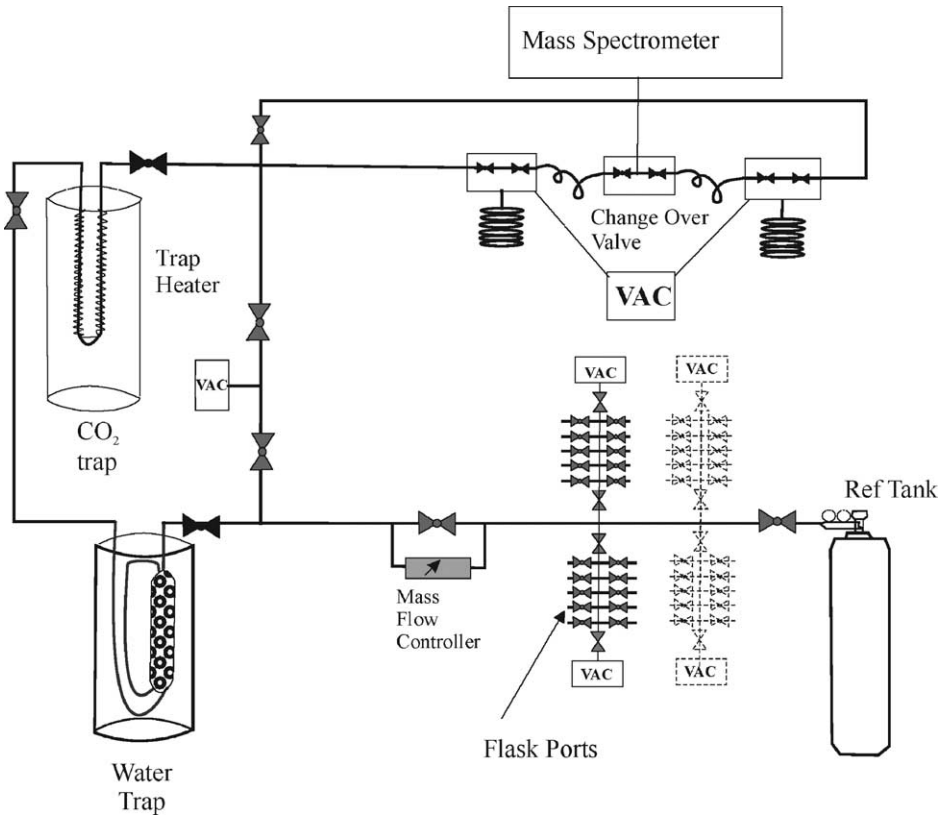

Fig. 5. Schematics of the CO_2 extraction system at INSTAAR (Boulder, CO) comprising flask manifold, water trap, CO_2 trap and inlet connection to the mass spectrometer (redrawn after White et al. [42]).

Table 1
Comparison of experimental parameters for extraction of CO_2 from air and isotope analysis in three laboratories

Parameters	Laboratories		
	NOAA-CMDL (Boulder, CO, USA)	CSIRO (Aspendale, Australia)	ISOLAB/BGC (Jena, Germany)
Material and design of cold traps	Glass, multiple loop	Glass (1982–1990), stainless steel (since 1990), multiple loop	Stainless steel and gold, concentric tubes
Number of traps	2	2 (or 3)	2
Micro volume	No	Yes	No
Flow rate (mL min^{-1})	40	4	60
Volume of sample air required for analysis (mL)	400	20–40	600
Mass spectrometer	VG SIRA Series 2 (1989–1996), Micromass Optima (since 1996)	VG602D (1982–1990), MAT252 (since 1991)	MAT252

weight and the mass spectrometer cannot distinguish between them (complete separation of the isobaric ions would require a working resolution in excess of 5000 for the three ion currents including high quality abundance sensitivity properties of the MS). If one is interested in the $\delta^{15}N$ of $\delta^{18}O$ of N_2O, separation of (neutral) CO_2 from N_2O may be done by absorbing CO_2 onto soda lime and collect the remaining N_2O for isotopic measurement. For analysis of $\delta^{13}C$ and $\delta^{18}O$ in CO_2, a separation procedure is a little more complex. It can be accomplished in three ways:

- Separate determination or measurement of the relative contributions and removal of $N_2O^{\bullet+}$ from the CO_2 signal using a mass balance correction.
- Physical removal of N_2O from CO_2 by converting N_2O to N_2 prior to measurement. This is achieved by passing the sample gas through a reducing agent (copper at 500 °C).
- Physical separation of CO_2 and N_2O using a gas chromatograph coupled online to an isotope ratio mass spectrometer.

The mass balance correction depends on a precise determination of the relative mixing ratios of the gases. The reducing agent approach can cause fractionation of the $^{18}O/^{16}O$ signature during the high temperature chemical reaction. The third approach of using a gas chromatograph for separating CO_2 from N_2O occurs without isotopic alteration [34,46]. This technique is capable of generating reproducible results with a precision of 0.05 and 0.08‰, respectively for carbon and oxygen isotopes in case of air CO_2 (which often is not sufficient for data interpretation). For reasons of precision, most laboratories routinely measuring the isotopic composition of CO_2 in air samples remove the $N_2O^{\bullet+}$ contribution to the $CO_2^{\bullet+}$ ion currents [47,48] using the mass balance correction approach. Possible isotopic variations in N_2O have little influence and are neglected in this case.

2.5.2. Analysis of air trapped in ice cores

For obtaining an ice core trace gas concentration and isotopic record, trapped air must be released from the ice sample, thereby carefully maintaining the quantitative composition. The ice is either molten for complete trace gas extraction (suitable for most trace gases, but not for CO_2) or it is mechanically crushed or ground at −20 °C under vacuum [49,50]. The air escaping from the bubbles is then collected by condensation at 14 K. Because not all bubbles are opened, extraction efficiency for the crushing technique is generally only 80–90%. After crushing, a small amount of the evolved gas is used for gas chromatographic determination. For CO_2 concentration the measurement precision is approximately 3 ppm. The major part of the sample gas is used for isotopic analysis. Here, CO_2 (together with N_2O) is quantitatively separated from the remainder of the sample at −196 °C in a metal vacuum line. The results are corrected for the isobaric interference of N_2O. Accuracy of the $\delta^{13}C$ results is about 0.1‰, as determined by analysing artificial CO_2 in air mixtures and from the scatter of the results around the smooth line. In order to increase the resolution of $\delta^{13}C$ records attempts are made to lower the amount of ice consumed without compromising precision.

Conventional offline techniques require relatively large amounts of ice. A new combined technique of gas chromatography and mass spectrometry has recently been introduced [51] which allows to work with drastically reduced sample amounts. The corresponding 5–10 g of ice contain only 0.5–1 mL S.T.P. of air or 0.1–0.2 μL of CO_2. The main components of the system are shown in Fig. 6a. In short, a stainless steel needle cracker is connected online with an isotope ratio mass spectrometer. Cracking of ice is done around −30 °C. From the cracker the gas expands through a water trap (−70 °C) into a larger stainless steel container (700 mL) from where it is flushed out with helium for isotopic analysis using a modified Finnigan MAT Precon system [52] (Fig. 6b). CO_2 is removed from the carrier gas in a small trap and frozen onto the column head prior to low flow (2 mL min^{-1}) gas chromatographic separation and online isotopic analysis. Correction for N_2O is not necessary in this case due to the separation of the two gases on the GC-column. Accuracy of the $\delta^{13}C$ results is about 0.1‰, as determined by analysing artificial CO_2 in air mixtures and from the scatter of the results around the smooth line.

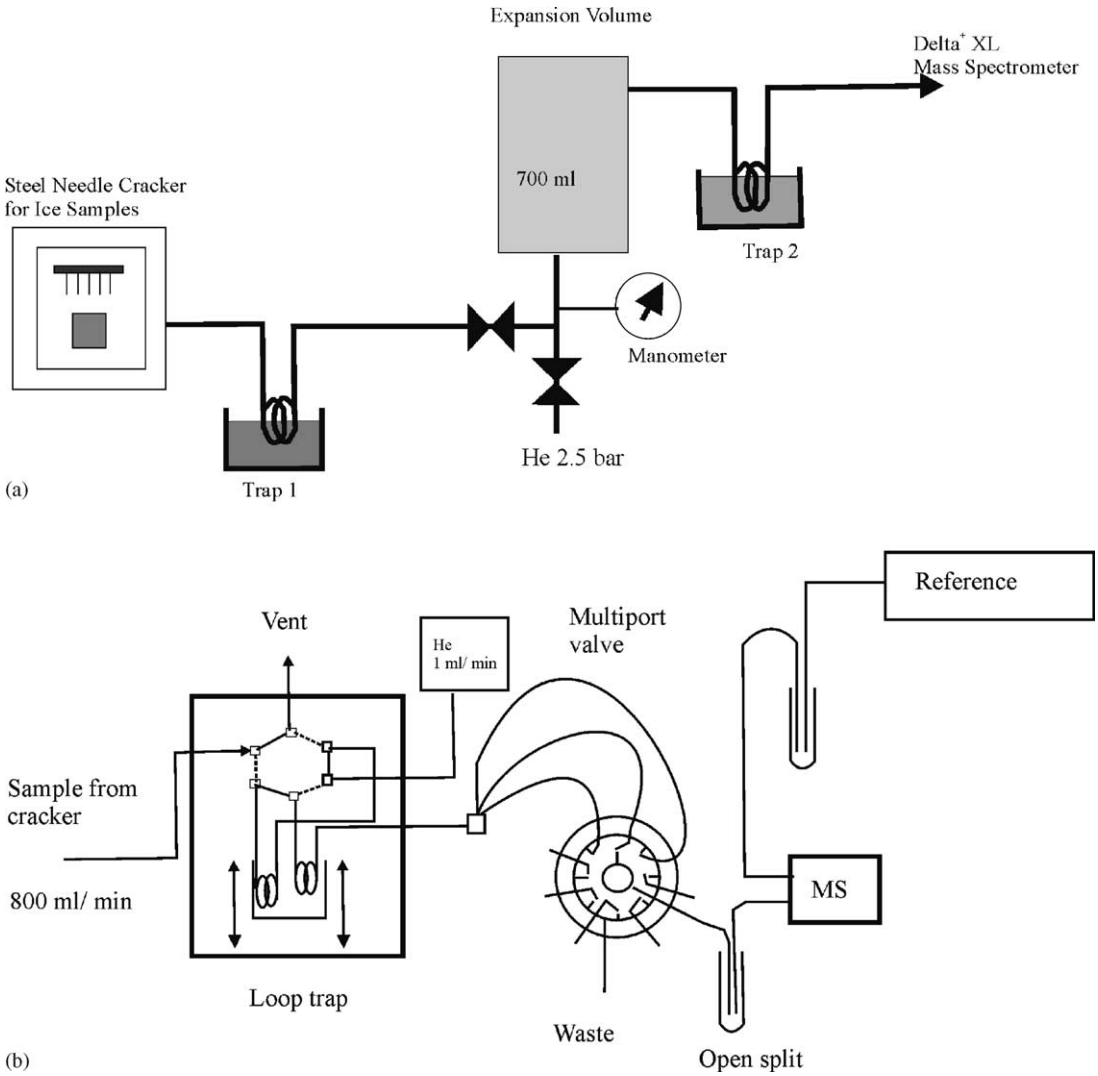

Fig. 6. (a) Preparation system for releasing CO_2 from air trapped in ice core samples comprising ice crusher, water trap and expansion volume (reproduced after Leuenberger and Huber [39]). (b) Pre-concentration system for $\delta^{13}C$ measurement comprising a multi-port valve with three capillaries of different length to split the CO_2 gas stream sequentially into three similar fluxes with a time lag of about 50 s each. This method allows enhanced precision of the measurements [39].

2.5.3. Stable isotopes determination in carbonate samples

For determining paleotemperatures from sediments, $^{18}O/^{16}O$ ratios of carbonate shells must be recovered with high precision. This is usually done by reaction of the carbonate with phosphoric acid under constant experimental conditions. The technique has been introducted by McCrea at the beginning of the 1950s [53] and used extensively since for paleoclimatic reconstruction. McCrea's original extraction system was made from glass and is shown in Fig. 7a. The reaction vessel containing the powdered carbonate (40–100 mg) in the main tube and the acid in the side arm can be evacuated, then tilted to pour the acid onto the carbonate. Reaction of acid and carbonate then generates CO_2 which expands into the evacuated

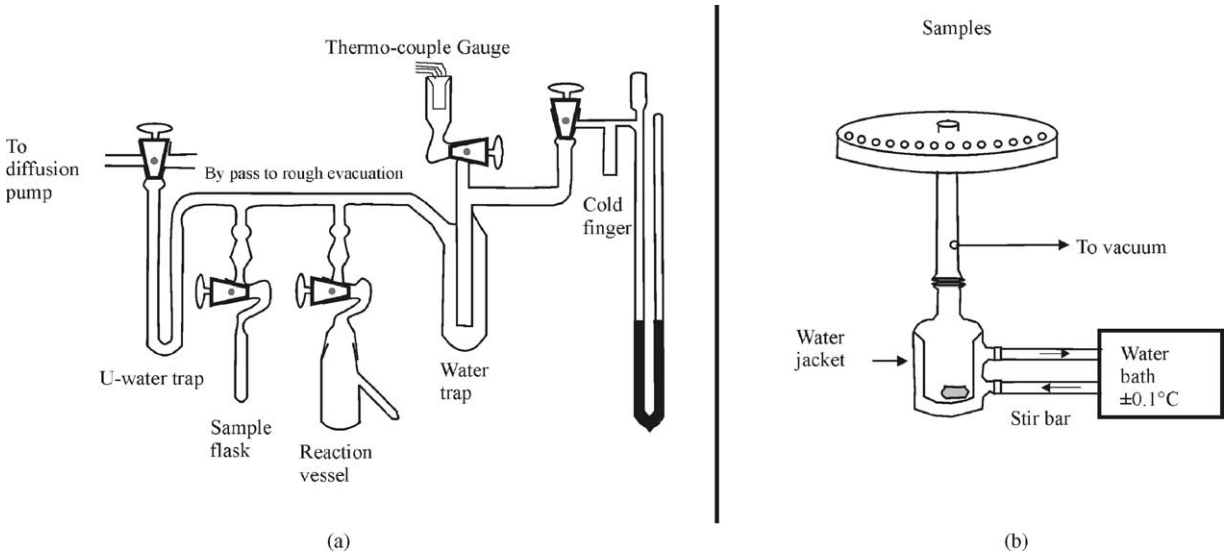

Fig. 7. (a) Extraction system used by McCrea (in 1950) for CO_2 extraction from carbonate samples [53]. (b) Common acid bath method showing the sample dropping mechanism sequentially into a common acid bath from a carousel. CO_2 evolved after reaction are frozen using a trapping mechanism (not shown in the diagram) (reproduced after Swart et al. [56]).

system and is subsequently condensed into the U-trap using liquid nitrogen. The carbon dioxide yield is measured with a manometer before final transfer to a sample tube for mass spectrometric analysis. Repeat analysis can be made with a precision of about 0.1‰ for both $\delta^{18}O$ and $\delta^{13}C$. Based on the experiments of McCrea it was concluded that isotopic fidelity can best be obtained by using a procedure in which the carbonate sample reacts with 100% H_3PO_4 at 25 °C, with the product CO_2 being retained in the reaction vessel until dissolution is complete. Phosphoric acid was ideal for this purpose because it has a very low vapour pressure and, in contrast to aqueous HCl or H_2SO_4, does not contribute oxygen to the reaction product. This method is generally regarded as the classical approach. Subsequent work has modified the method mainly to handle smaller amounts of sample. Shackleton and Opdyke [54] and Mathews et al. [55] used 100% H_3PO_4 at 50 °C, immediate separation of CO_2 from the online extraction system and a direct connection to the mass spectrometer. Swart et al. [56] compared an alternative, common acid bath method with the classical approach (Fig. 7b). The common acid bath method involves the use of an aliquot of acid into which all samples of a series are dropped and reacted. The carbon dioxide produced is continuously removed during the reaction using liquid nitrogen. In order to decrease the reaction times and to degas the acid higher temperatures up to 90 °C are employed. In all cases where the reaction temperature differs from 25 °C, the temperature dependence of the reaction must be considered and the results must be corrected [56].

3. Stable isotope signatures in climate research

3.1. Terrestrial versus marine deposition, $\delta^{13}C$ in air-CO_2

A precise determination of the isotopic composition can help separate CO_2 fluxes into terrestrial and marine components. To follow the fate of CO_2 in the atmosphere, Keeling et al. [8] for example compared variations in the concentration of atmospheric CO_2 with variations in the $^{13}C/^{12}C$ isotopic ratio of this gas in air collected at both Mauna Loa Observatory and South Pole (Fig. 8). As discussed above, the isotopic fractionation of carbon in the major pathways

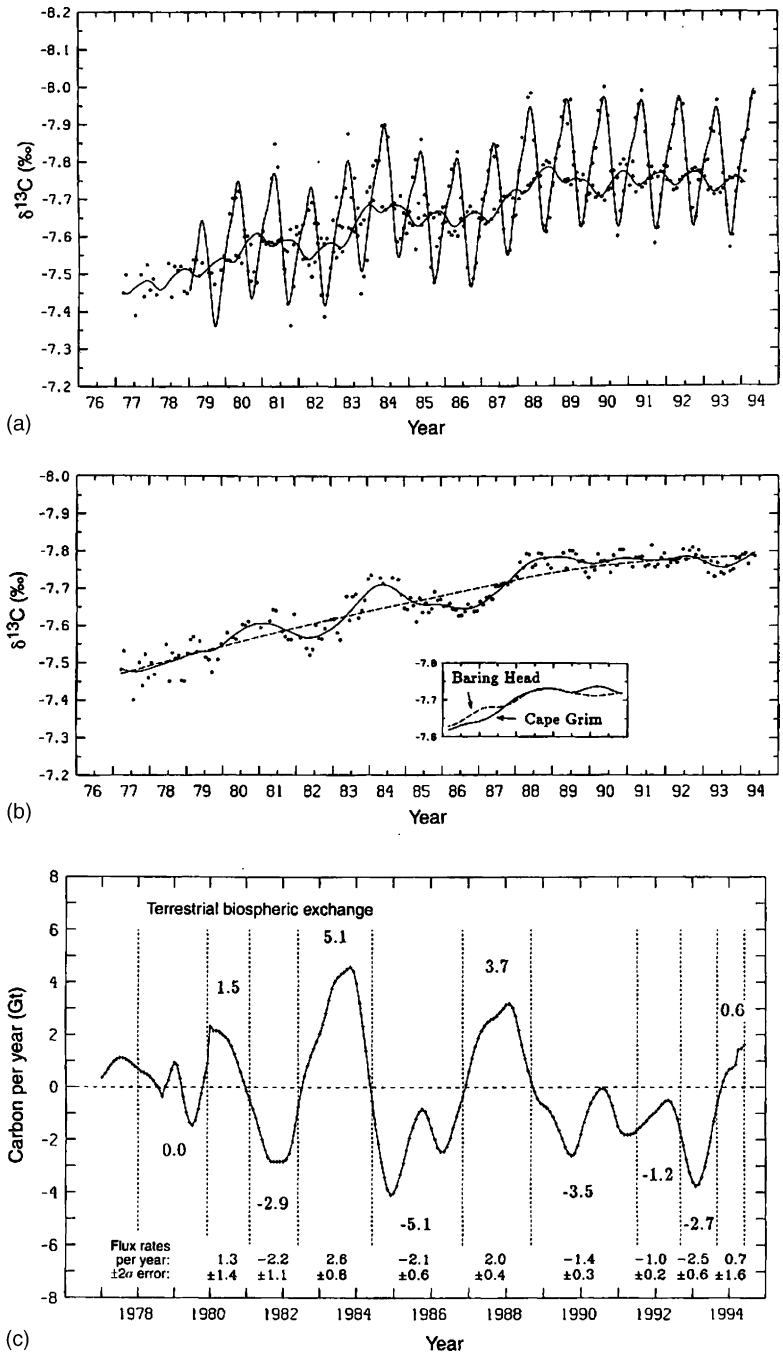

Fig. 8. $\delta^{13}C$ of atmospheric CO_2 from 1977 to 1994 together with inter annual exchange of atmospheric CO_2 with world ocean and terrestrial biosphere. (a) The $\delta^{13}C$ records of CO_2 from Mauna Loa Observatory and the South Pole exhibit pronounced seasonal cycles. (b) Average of (a) after seasonal adjustment. (c) Estimates of exchange of CO_2 by the terrestrial biosphere with the atmosphere, determined by a double de-convolution method. (d) Residual exchange of CO_2 with the ocean obtained from allowing for oceanic absorption of CO_2 predicted in response to industrial CO_2 emission and isotopic disequilibrium attending that response (Keeling et al. [8], reproduced with permission from *Nature*, http://www.nature.com/).

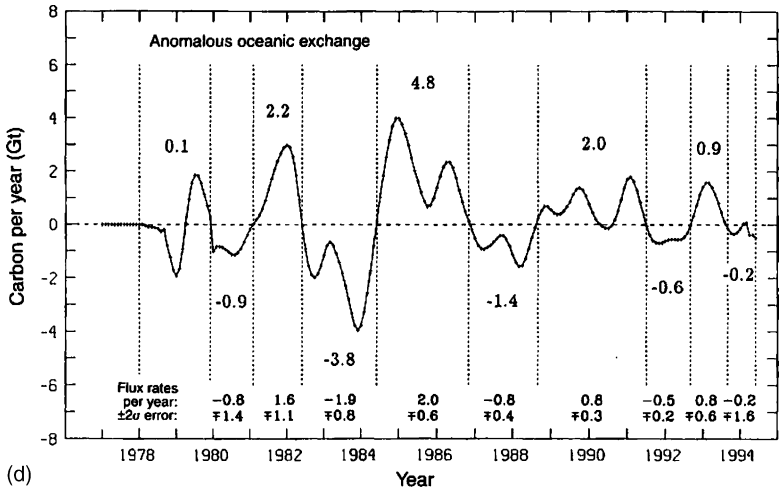

Fig. 8. (*Continued*).

of the global carbon cycle allows to separate contributions to the atmospheric CO_2 record from the terrestrial biosphere and from the oceans. Fig. 8c and d show that the inferred biosphere and oceanic fluxes have tended to oppose each other. Increases in biosphere sources and anomalous oceanic sinks occur at times of rising CO_2 anomaly and vice versa. However, there was an exception following the mid-year 1991. During that period sinks are indicated for both fluxes, perhaps a rare event, showing anomalous conditions due to either the eruption of Mt. Pinatubo[3] or to the presence of a weak El Niño[4] event during both 1992 and 1993 in the Tropical Pacific [8]. This study makes use of $\delta^{13}C$ values together with the measured CO_2 mole fractions for extracting information about flux variations (Fig. 8).

In spite of the experimental achievements measurement precision is still a limiting factor for more rigorous data interpretation: current fossil fuel emissions of about 6 Gt C per year result in a long term change of the CO_2 mixing ratio in the atmosphere of about 1.5 ppm per year. $\delta^{13}C$ of CO_2 changes about 0.02‰ per year. While CO_2 mixing ratio analyses can be made with a typical precision of 0.1 ppm (which is less than 1/15th of the annual change), demonstrated precisions for $\delta^{13}C$ are at best near 0.01‰, i.e., approximately half the annual trend. For a reasonable partitioning of net oceanic versus terrestrial fluxes from a time series analysis of $^{13}CO_2$ in air samples Keeling et al. [8] and Francey et al. [57] have formulated an inter-laboratory precision goal of 0.01‰ for $\delta^{13}C$.

The role of data uncertainty, both in concentration measurement and isotope ratios of CO_2 in air samples for deriving global carbon fluxes has been discussed in further details in Rayner et al. [58].

3.2. $\delta^{18}O$ in atmospheric CO_2

The potential of $\delta^{18}O$ measurements in air samples may have been underestimated in the past. Today it is anticipated that $\delta^{18}O$ analyses of CO_2 will enable us to better understand the partitioning of global net CO_2 exchange fluxes on land into its photosynthetic and respiration components. The potential of this approach was first noted by Francey and Tans [22] followed by

[3] A June 1991 volcanic eruption on a mid Pacific Island close to the Phillipines contributing large amounts of dust to the stratosphere and of mantle CO_2 to the atmosphere.

[4] El Niño is a climatic oscillation in the equatorial Pacific ocean associated with large sea surface water temperature changes. In these events the ocean becomes a sink of CO_2, whereas the terrestrial biosphere acts as a source due to wild fires and changes in soil respiration.

more rigorous investigations showing an appreciable $\delta^{18}O$ signal (latitudinal gradients and seasonal variations) connected to biospheric activity in the global atmosphere as well as consistency in the global scale ^{18}O mass balance [22,59–61]. These studies also reiterated the critical need to reduce the uncertainty associated with oxygen isotope measurements. In order to extract a maximum of information, high precision and accuracy in determining $\delta^{13}C$ and $\delta^{18}O$ values over decadal or greater timescales is important. Only a handful of laboratories have to date demonstrated an ability to measure $\delta^{13}C$ from CO_2 in air with long term precision of 0.015‰. Inter-laboratory precision in case of oxygen is still poor compared to an expected target precision of 0.03‰ in $\delta^{18}O$ [62].

3.3. Paleoclimate reconstruction

While it has been possible for the past 50 years to measure the CO_2 mixing ratio and the isotopic composition of air samples directly, this information must be recovered by more indirect means for the more distant past. Much of our quantitative knowledge of climate fluctuation in the past has been derived from records preserved in ice sheets and deep sea sediments.

The main palaeoclimatic indicators have been the abundance ratios of the oxygen isotopes in water as well as oxygen and carbon isotopes in carbonates. The difference in physical properties caused by the mass difference leads to temperature dependent isotopic fractionations during phase changes and chemical reactions. This allows the oxygen isotopic ratio to be used as a tracer for studying: (1) climate and the hydrological cycle, (2) carbonate precipitation and dissolution and (3) photosynthesis and related process. Products formed as a result of interaction between water and its surrounding can be preserved over time and can, with the isotopic signature, serve as a proxy record of past climate change.

Different types of palaeoclimatic records from ice sheets and ice caps, peat bogs, lake and ocean sediments, loess deposits, speleothems and tree rings from different parts of the world provide a mosaic of well documented local responses to global climate changes. But for a meaningful comparison it is essential that the timing of the different records is accurately known and that differences in response time for different records are considered during interpretation.

3.3.1. Water and air trapped in ice cores

The water oxygen and hydrogen isotopic composition of ice cores have preserved palaeoclimatic information such as local temperatures and precipitation rate, moisture source conditions, etc., whereas trapped air within ice cores directly provides atmospheric trace gas concentrations and indirectly allows to estimate aerosol fluxes of marine, volcanic, terrestrial, cosmogenic and anthropogenic origin [50,57,63]. The ice-drilling project undertaken in the framework of a long term collaboration between Russia, the US and France at the Russian Vostok Station in East Antarctica has provided a wealth of information of changes in climate and atmospheric trace gas and aerosol composition over the past four glacial–interglacial cycles (i.e., for the last 400,000 years [64]).

The data plotted in Fig. 9a and b show $\delta^{13}C$ results obtained from trapped air in an Antarctic ice core [50]. It represents one of the earliest results from ice cores exhibiting a general increase in CO_2 concentration with time since 1750 together with a decrease in $\delta^{13}C$ values. Using these data it was possible to directly compare measurements of CO_2 concentrations in air obtained at Mauna Loa since 1958 by Keeling et al. [8] with the longer term ice core archive record from Antarctica. The average $\delta^{13}C$ value of samples before 1800 A.D. is −6.41‰ in the ice core. This observation is in excellent agreement with the extrapolated pre-industrial mean value for the South Pole inferred from direct air sampling (−6.44‰) and therefore adds confidence to using ice cores as a tool for palaeoclimatic investigations.

Continuous ice cores for studying past climatic events are also available from Greenland or alpine glaciers [65]. Dansgaard et al. [66] and Johnsen et al. [67] have utilised oxygen isotope measurements in ice cores from Greenland to reconstruct surface temperature exceeding the last 100,000 years. Similarly,

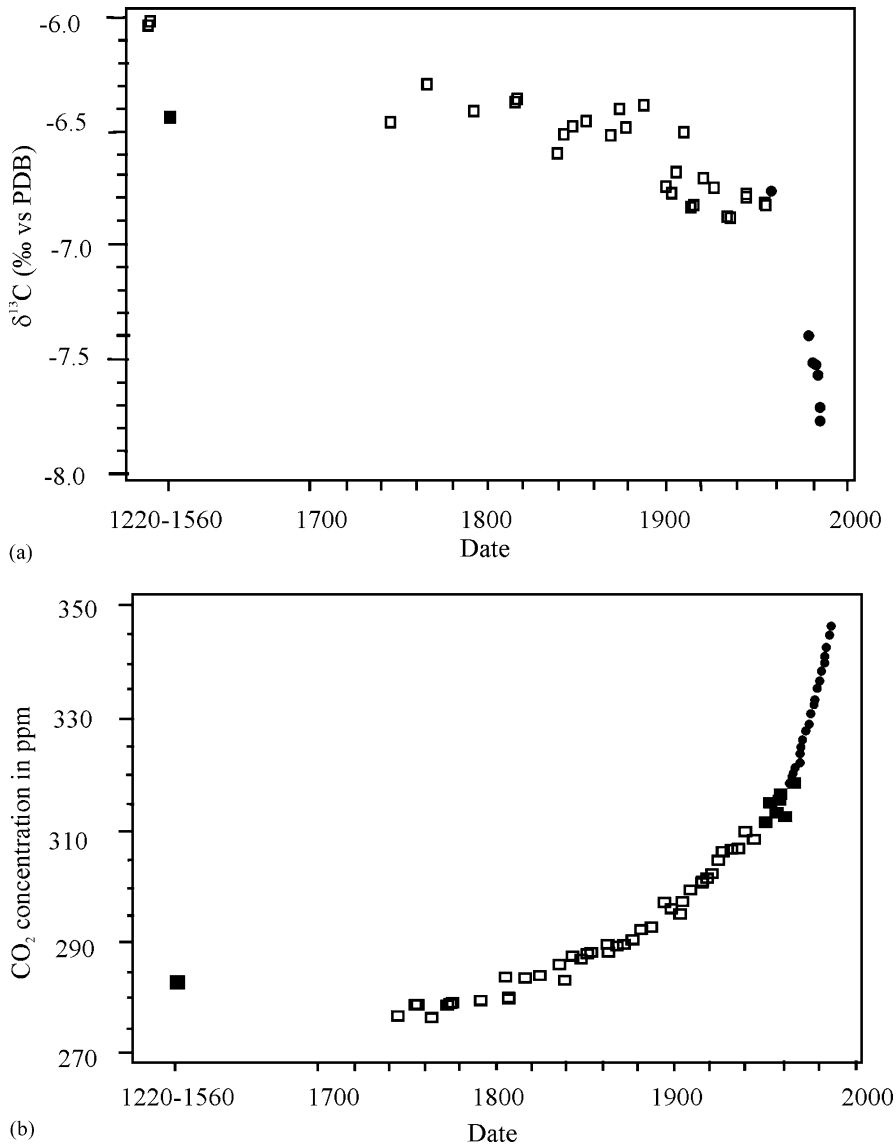

Fig. 9. $\delta^{13}C$ values of CO_2 from air samples (a) and CO_2 concentration in air (b) extracted from ice cores from Siple Station Antarctica (□) and from South Pole Station (■). Also shown are results from direct atmospheric samples at Mauna Loa (Friedli et al. [50], reproduced with permission from *Nature*, http://www.nature.com/). Please note: the original PDB scale has been superseded by the VPDB scale. The numerical values are not affected by this.

Lorius et al. [68] and more recently Petit et al. [64] have used $\delta^{18}O$ measurements from the above mentioned Vostok ice core (3310 m thick ice deposit) to reconstruct estimates of surface temperature for more than the last 400,000 years (Fig. 10). Temperature reconstruction (trace b) is shown for the Vostok ice core along with observed variation in trace gas concentration. Prominent features of this record are the large amplitude and the sudden change in temperature between glacial and interglacial periods, estimated at as

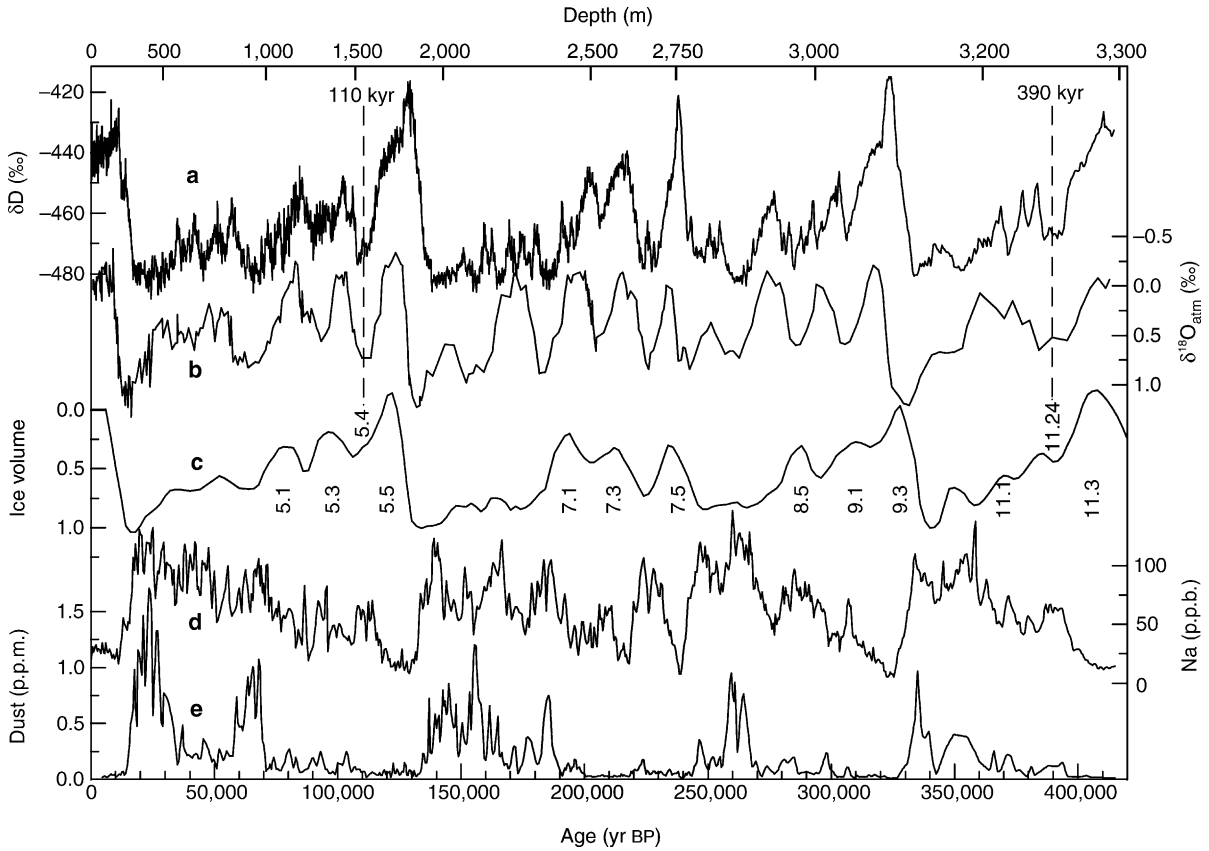

Fig. 10. Variation of CO_2, CH_4 and $\delta^{18}O$ obtained from the analysis of Vostok ice core samples, East Antarctica. Also shown are the estimates of temperature and insolation changes (Petit et al. [64], reproduced with permission from *Nature*, http://www.nature.com/).

much as 8–12 °C. There are four glacial cycles characterised by low CO_2 and CH_4 concentrations in the atmosphere and ^{18}O-enrichment in ice-H_2O. The third and fourth climatic cycles were of a shorter duration than the first two. These features are also found in deep sea carbonate records. Each glacial–interglacial cycle consists of a saw-tooth sequence of warm interglacial events, followed by increasingly colder interstadial events, and ending with an abrupt return towards the next interglacial. The data in Fig. 10e provide estimates of insolation changes at 65° North. The warmest time interval at 200–230 ka was slightly warmer than the Holocene [69]. These observations may be important in the context of the continued contemporary CO_2 increase and possible consequences for the future of the Earth's climate.

3.4. Paleotemperatures for geological time scales from carbonate minerals

Ocean sediment carbonates are comprised of phytoplankton shells known as foraminifera and ostracods.[5] Individually, they are microscopic in size, but together they contribute one of the major components of the shallow ocean chemical system. The chemistry of aqueous carbonate formation arises from the saturation with HCO_3^- and Ca^{2+} ions. The bicarbonate ion is formed by dissolution of CO_2 which has evolved from various processes including respiration, degassing from subsurface sources and decomposition

[5] Foraminifera are protozoans and ostracods are crustaceans like crabs and lobsters.

of dead organic matter. The calcium ion mainly originates from weathering of the continental platform. The microscopic animals secret a shell around their body as a protective covering, thereby effectively decreasing the concentration of HCO_3^- and Ca^{2+} ions in the surrounding water. After death the animal shells sink down to the ocean floor and remain preserved in sediments. The shells are made up of two types of carbonate mineral; calcite and its precursor aragonite. Calcite and aragonite are enriched in ^{18}O compared to the water from which they were precipitated. When the reaction takes place in isotopic equilibrium, the $\delta^{18}O$ value of the calcite can be related to $\delta^{18}O$ of sea water and the temperature (in °C) by [53,70]:

$$T = 16.9 - 4.2(\delta_c - \delta_w) + 0.13(\delta_c - \delta_w)^2$$

where δ_c is the $\delta^{18}O$ value of CO_2 prepared by reacting calcite with 100% H_3PO_4 at 25 °C and δ_w is $\delta^{18}O$ of CO_2 in equilibrium with water at 25 °C. Both δ-values are on the same (VSMOW) scale.

The oxygen isotopic palaeo-thermometer is based on the assumption that biogenic calcite and aragonite are precipitated in isotopic equilibrium with sea water. This requirement is met only by a few carbonate secreting organisms including molluscs and foraminifera. For shells from these organisms, for every 1 °C rise in water temperature there is 0.25‰ drop in $\delta^{18}O$ of carbonate in isotopic equilibrium with that water. Decreasing $\delta^{18}O$ values in shell carbonate thus indicate increasing temperatures if $\delta^{18}O$ of the water were to have remained constant. This is obviously not always the case, especially during glacial/interglacial periods because of the large effect of ice piling up in the polar areas. More information is needed to decouple the $\delta^{18}O$ source from the temperature signal. In some cases this conflict can be resolved by simultaneous measurement of trace elemental ratios like Sr/Ca. For corals, such ratios are independent of salinity which reflects the source water oxygen isotopic composition. Hence, for coral cores found in proximity to the cores used for paleotemperature determination, a correction is possible and unambiguous temperatures can be derived [71].

The carbon isotopic composition ($\delta^{13}C$) is determined by CO_2 forming the HCO_3^- ion. The source of CO_2 is mainly respiration and decomposition of organic matter. Both these processes produce CO_2 of similar isotopic signature. In phytoplankton carbon isotopic composition is predominantly controlled by photosynthetic activity. Other factors like temperature are of minor significance. Therefore, variations of $\delta^{18}O$ and $\delta^{13}C$ in marine planktonic foraminifera can potentially be used to understand the variability of photosynthetic activity in the past.

Despite the potentially complex array of controls, natural waters tend to show a characteristic range of carbon and oxygen isotope values which in turn are mimicked or tracked by the carbonate minerals precipitated from them. Consequently, plots of $\delta^{18}O$ versus $\delta^{13}C$ for carbonate materials can help identify their depositional and/or diagenetic environment(s). Using stable isotope analysis of carbonates enables us to study the conditions of deposition and to estimate the temperature of formation [53].

3.5. The deep sea stable isotope record

Oxygen and carbon isotope data for bottom dwelling deep sea foraminfera from over 40 Deep Sea Drilling Project (DSDP) and Ocean Drill Project (ODP) sites cover a large part of the Cenozoic period [72]. All data have been collected from the literature and compiled into a single deep sea isotope record (Fig. 11). Numerical ages are given relative to the standard geomagnetic polarity time scale for the Cenozoic [73]. To facilitate visualisation the data have been smoothed and curve fitted using a locally weighted mean. The oxygen isotope data provide constraints on the evolution of deep sea temperature and continental ice volume. This is because deep ocean waters are derived primarily from cooling and sinking of water in polar regions and the deep sea surface temperature data also double as a time averaged record of high latitude sea surface temperature (SST). On the other hand, the deep sea carbon data provide information about the nature of global carbon cycle fluctuations and changes in deep sea circulation patterns that

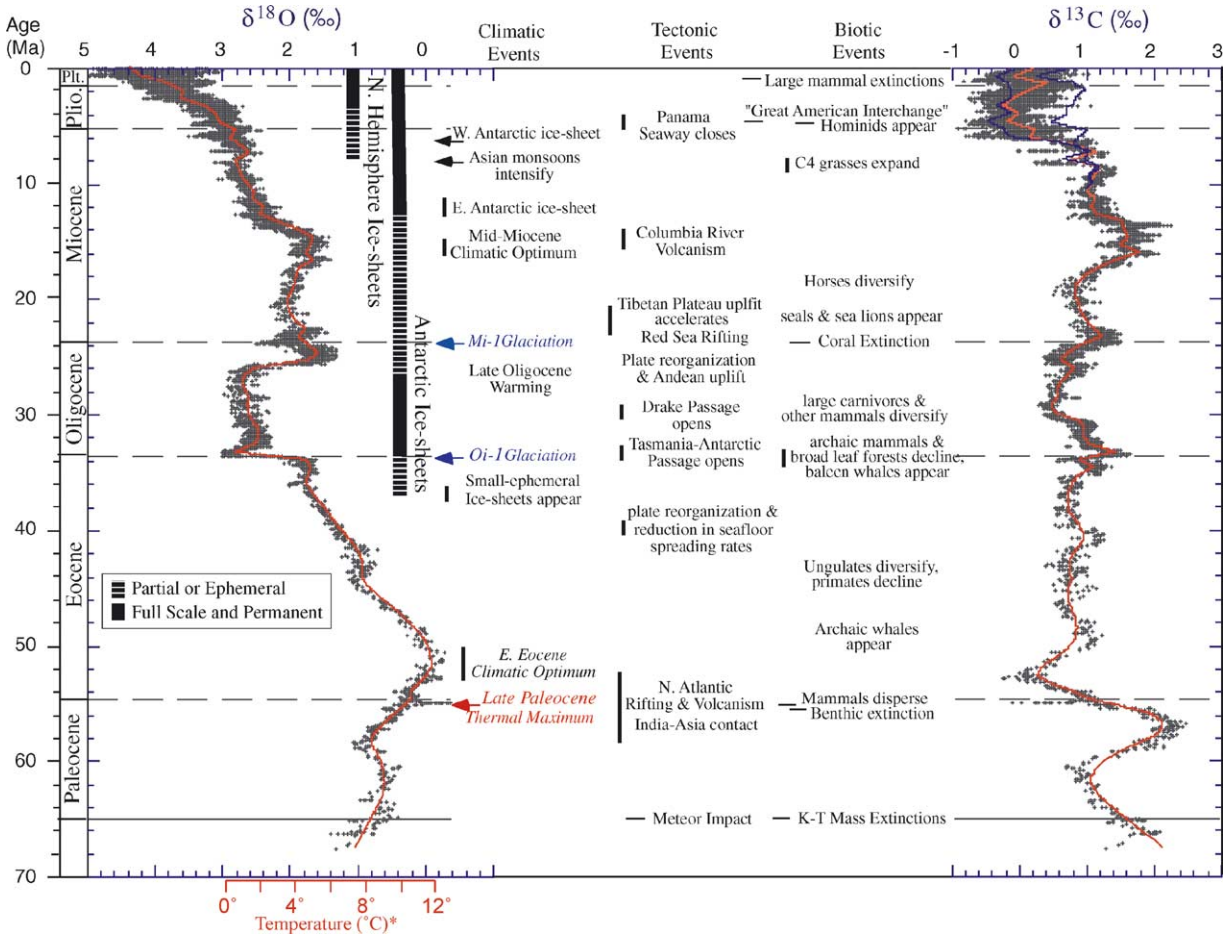

Fig. 11. Global deep sea oxygen and carbon isotope records based on data for more than 40 Deep Sea Drilling Project and Ocean Drilling Project sites (Zachos et al. [72], reproduced with permission from *Science Magazine*, http://www.sciencemag.org/). Some key tectonic and biotic events are marked in the diagram. (*) The temperature scale has been inferred from the $\delta^{18}O$ record assuming an ice-free ocean with $\delta^{18}O \sim 12‰$ w.r.t. VSMOW [72].

might produce or arise from climatic changes. The $\delta^{18}O$ and $\delta^{13}C$ records in Fig. 11 demonstrate several major and some minor episodes of climatic changes during last 70 Ma. The sudden drop in isotopic ratios (both for carbon and oxygen isotopes) denotes effects caused by warming processes. These episodes are denoted by arrows indicating geological periods with high ocean temperature. Many of these trends are tectonically controlled and reflect sudden input of hydrothermal fluids from deep inside the Earth. The impact of the Earth's tectonic activity caused major shifts in climate and played an important role in providing conducive conditions for biotic evolution.

The marine carbon isotopic composition was considered an invariant quantity (∼0‰ w.r.t. VPDB) until 1980 when it was realised that oscillating secular signals are preserved in stratigraphic records [74–77] marking the times of major global changes in Earth's history. In contrast to the below-discussed oxygen isotopes, the pristine nature of this $\delta^{13}C$ carbonate secular trend has not been criticised. Diagenetic alteration of carbonates occurs in a system with a low water/rock

ratio for carbon, and a high ratio for oxygen [78,79]. Diagenetic stabilisation of carbonates therefore results in transport of carbon from a precursor to a successor mineral phase. Oscillations in the $\delta^{13}C$ carbonate trend can thus be utilised for correlation and isotope stratigraphy [80,81]. This proxy, however, is subject to several limitations as compared to Sr isotopes. The major difference arises from the fact that $\delta^{13}C$ of ocean carbonate at any given time can show a considerable spread of values due to spatial variability of oceanic $\delta^{13}C$ [82] and due to biological factors present during shell formation [83]. The complications arise not so much during logging of a single well or a profile, but can become considerable when isolated sedimentary sequences or wells are compared. Nonetheless, large peaks can serve as correlation markers, particularly in the Precambrian [84]. In addition, the secular $\delta^{13}C$ carbonate trend can be used as an indicator for determining oceanic palaeo-productivity and preservation patterns, ancient pCO_2 and pO_2 states, and similar palaeo-environmental phenomena [85–87]. Fig. 12, shows combined $\delta^{13}C$ data from limestone and shell portions plotted against age as compiled in Veizer et al. [87]. This plot shows the secular variation as an increase in $\delta^{13}C$ throughout the Paleozoic, followed by an abrupt decline and subsequent oscillations around the present-day value in the course of the Mesozoic and Cenozoic. This variation can be compared with Sr isotope ratio variations during the Phanerozoic. The running mean based on these values was calculated for 5 Ma incremental shifts [87] to make it useful for global bio-stratigraphic correlation. The bands around this mean incorporate 68 and 95% of all measured samples, respectively. Considering the global nature of the data set, with samples originating from five continents and a multitude of sedimentary basins,

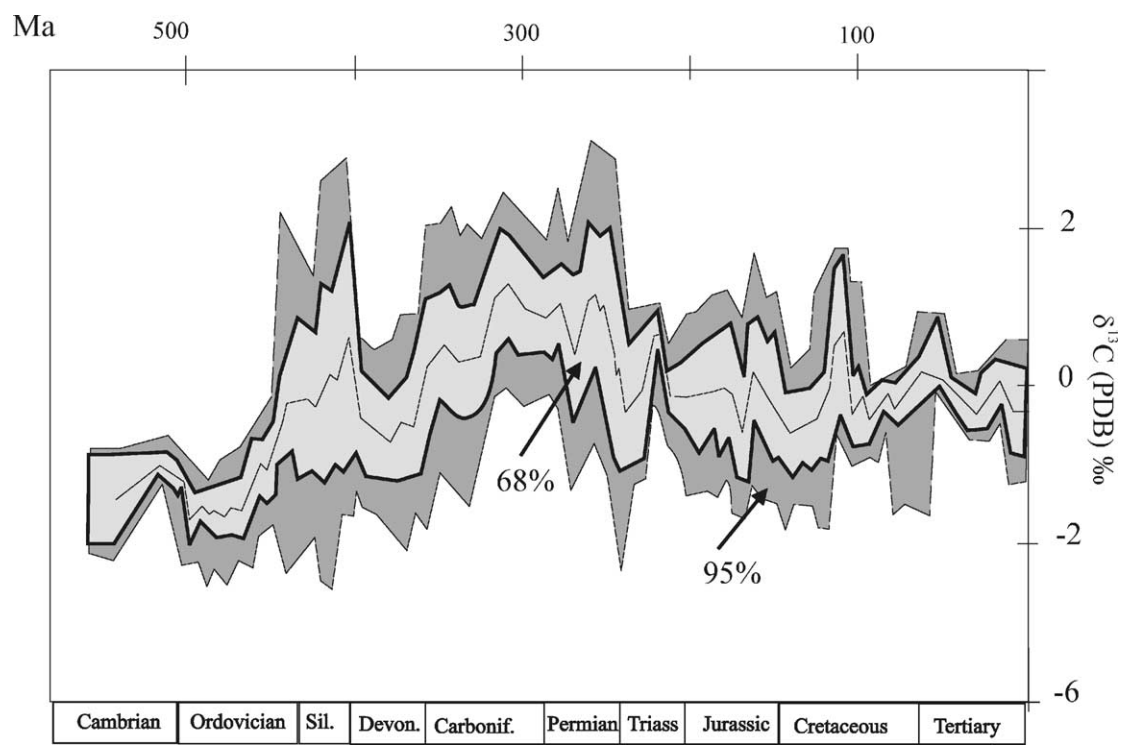

Fig. 12. Phanerozoic $\delta^{13}C$ trend of the world ocean. The running mean is based on 20 Ma windows and 5 Ma forward step. The shaded area around the running mean includes 68 and 95% of all data, respectively (modified after Veizer et al. [87]). See also note in the caption to Fig. 9.

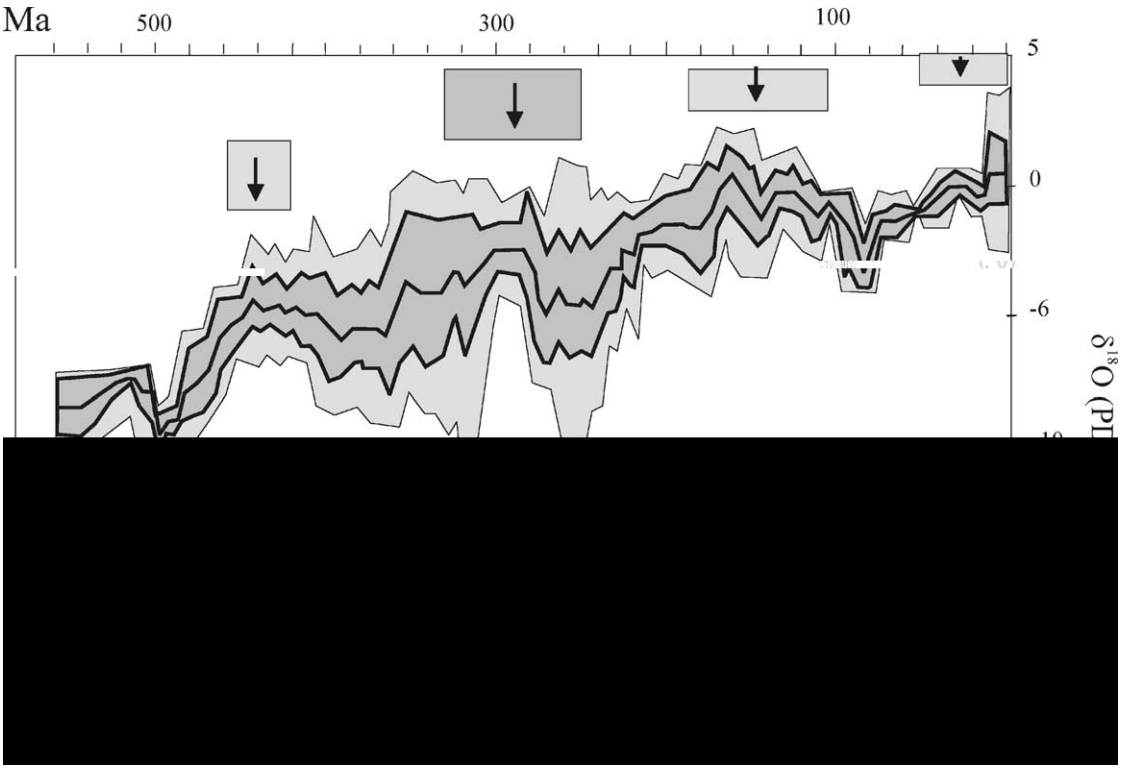

Fig. 13. Phanerozoic $\delta^{18}O$ trend in the world ocean derived from low magnesium calcite shells, believed to preserve the $\delta^{18}O$ composition. Glaciation and cold times are marked (redrawn after Veizer et al. [87]). See also the note in the caption to Fig. 9.

the observed peaks are of global significance and denote episodes of abrupt climatic change.

The observed $\delta^{18}O$ trend in marine carbonates is similar to the variation in carbon isotope ratios. Global data sets comprising a statistically meaningful number of samples when plotted against time show a trend of increasing $\delta^{18}O$ values, from about −8‰ at the onset of the Phanerozoic to about 0‰ at present. In spite of a signal ambiguity probably caused by natural variability the statistical treatment of the data set exhibits an oscillation with a frequency of 150 Ma, coinciding with cold intervals during glaciations (Fig. 13). These periods are marked by an increase in $\delta^{18}O$.

3.6. Reconstruction of short term sea surface temperatures from Sr/Ca ratios and $\delta^{18}O$ of corals

A reconstruction of past sea surface temperatures (SST) and of variations of the $\delta^{18}O$ in sea water became possible with coupled $\delta^{18}O$ and Sr/Ca analysis[6] of coral skeletons[7] [71,88] This is because the $\delta^{18}O$ composition of carbonate precipitating from water under equilibrium is governed by both, temperature and salinity changes.[8] Due to evaporation processes, leaving the electrolytes and enriching the heavier isotopomers in the liquid phase, salinity and $\delta^{18}O$ are positively correlated in the world's oceans—as salinity increases so does the amount of the heavier isotope [89]. By contrast, variations in the Sr/Ca

[6] The analysis of Sr/Ca ratios can be made using thermal ionization MS (TIMS) or ICP-MS.

[7] As living animals, corals provide habitats for many other organisms. The breakdown of their skeletons after death provides material for redistribution and consolidation into the reef framework.

[8] Ocean water has a salinity of approximately 35,000 ppm, in other words: ocean water contains about 3.5% salt. Sometimes, salinity is expressed on a different scale. A common unit is the psu (practical salinity unit). 1000 ppm = 1 psu. Salinity is measured with a CTD instrument (CTD: conductivity, temperature, depth).

ratio of coral carbonate are independent of salinity changes. Therefore, combining $\delta^{18}O$ and Sr/Ca ratios allows the determination of past changes in sea-water $\delta^{18}O$ composition, which is useful to study variations in tropical hydrological cycles. The change in sea water $\delta^{18}O$ is defined by the differences between coral Sr/Ca and $\delta^{18}O$ curves (residual $\delta^{18}O$). Differences in sea water $\delta^{18}O$ should reflect changes in sea surface salinity (SSS) because rainfall on land is depleted in ^{18}O relative to sea water, while evaporation tends to enrich the surface ocean in ^{18}O [90].

Gagan and Chivas [91] studied $\delta^{18}O$ variations in sea-water from tropical regions by estimating the $\delta^{18}O$ residual from Sr/Ca and $\delta^{18}O$ data sets for *P. lutea* colonies growing in three different ocean environments including the Great Barrier Reef, the eastern Indian Ocean (Papua New Guinea) and the Indonesian seaways (Java). These test sites covered seasonal extremes in the tropical SST range (20–31 °C). For the austral winter dry season (when changes in SSS and presumably sea water $\delta^{18}O$ are negligible) being taken as a starting point, the $\delta^{18}O$-SST calibration for the Great Barrier Reef site was centred around a dry season salinity of 35.2 psu ($\delta^{18}O$ defined as 0‰). By comparison, the dry season coral $\delta^{18}O$ residuals for Java and Papua New Guinea were −0.40 and 0.35‰, respectively. The negative $\delta^{18}O$ residuals reflect the relatively low salinity water mass encompassing the warm pool region, where the input of ^{18}O depleted precipitation exceeds evaporation. Given that the average difference in salinity between the two warm pool sites and Orpheus Island in the Great Barrier Reef was ∼1.4 psu, the slope of $\delta^{18}O$/SSS relationship is ∼0.25–0.29‰. The $\delta^{18}O$/SSS slope from the above study is essentially the same as the one derived recently for a network of water sampling sites near reefs of the tropical Pacific of 0.27‰ [92]. The results suggest that the coral residual $\delta^{18}O$ proxy is capable of yielding an accurate reconstruction of relative differences in sea water $\delta^{18}O$ which, at least for Indo-Pacific reef settings, can be used to make inferences about salinity. It is now possible to investigate the potential for abrupt climate change in the Tropical Surface ocean via several deglacial to late Holocene coral palaeo-temperature records available from the south western Pacific region. Fig. 14 shows a compilation of paleo-SST estimates for corals collected from different tropical regions. The corals were dated using TIMS ^{230}Th, AMS ^{14}C or U/Th measured by alpha spectrometry. The results from well-preserved fossil corals from the tropical western Pacific and Atlantic suggest that temperatures during the mid stage of the last de-glaciations (10–14 ka) were 4–6 °C lower than today.

3.7. Reconstruction of carbon isotopic composition of atmospheric CO_2 from speleothems

Speleothems (stalagmites and stalagtites) have been used to retrieve continental palaeo-environmental information. Speleothems are calcium carbonate deposits from the ceiling and floor of ancient caves. They grow mainly under wet and warm environmental conditions. Oxygen isotopic composition of speleothems together with radiometric dating techniques have been used for the reconstruction of past precipitation and temperature patterns, mainly for glacial periods [93–99]. One of the important assumptions in using speleothem $\delta^{18}O$ to reconstruct climate is that inside the cave a relative humidity of 100% persisted during precipitation of the carbonate. Hence, uncertainties arise from the sampling location because this condition is never fulfilled in a natural cave over extended periods of time. In contrast, the carbon isotope composition can be used reliably for reconstructing the carbon isotopic composition of atmospheric CO_2. Baskaran and Krishnamurthy [100] demonstrated that $\delta^{13}O$ of speleothems from recent cave deposits exhibits a trend which closely parallels the $\delta^{13}C$ trend in atmospheric CO_2 at the time. Carbonate precipitation in speleothems involves dissolution of parent limestone by dissolved CO_2 in the percolating water and subsequent degassing of CO_2 from the solution or evaporation causing super saturation and subsequent deposition. CO_2 in ground water mainly arises from soil horizons, formed from soil respiration and atmospheric diffusion [101]. Provided

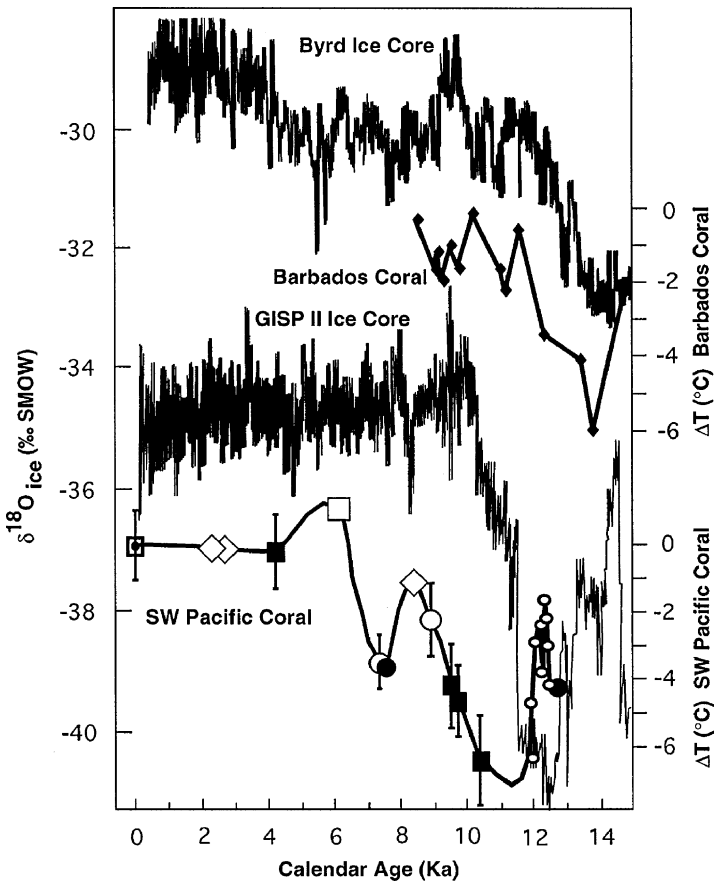

Fig. 14. Comparison of reconstructed sea surface temperatures for the south western Pacific and the tropical Atlantic. Also shown are the $\delta^{18}O$ records of the GISP II and Byrd polar ice cores. Sea surface temperature variations were obtained from $\delta^{18}O$ and Sr/Ca ratios in corals from equatorial regions. Sr/Ca ratios are from Papua New Guinea (○); Sr/Ca Vanuatu (■); Sr/Ca Seychelles, Tahiti (●); Sr/Ca of Great Barrier reef, Australia (□); $\delta^{18}O$ are from Papua New Guinea (◇) (reproduced after Gagan et al. [71]). Please note: the original SMOW scale has been superseded by the VSMOW scale. The numerical values are not affected by this.

the flux and isotopic composition of CO_2 originating from decomposing organic matter remain constant during speleothem formation the variation in isotopic composition of atmospheric CO_2 will be reflected in the resultant carbonate. Such variation in isotopic composition was observed in cave deposits (<200 years, San Saba County, TX, USA). This investigation showed an overall $\delta^{13}C$ decrease following the atmospheric trend for the past 70 years with an annual rate of −0.032‰, comparable to the direct atmospheric measurements [20].

3.8. $\delta^{13}C$, $\delta^{18}O$, temperature and tree rings

Living plants utilise water from precipitation and CO_2 from their respective environment to generate new organic material via photosynthesis. Consequently, the isotopic compositions of these source materials can be found in the plant, however, modified through natural fractionation processes (see also Fig. 1). Farquhar et al. [102] examined the $\delta^{13}C$ composition of leaf tissue and atmospheric CO_2 and observed a constant fractionation law between

them. This lead to the introduction of a model for ^{13}C discrimination associated with CO_2 uptake in C_3-photosynthesis [103]. The model indicates that ^{13}C discrimination is influenced by the ratio of the CO_2 concentration inside the leaf (C_i) and in the atmosphere (C_a) according to [102]:

$$\delta^{13}C_{plant} - \delta^{13}C_{atm} = e_d\left(\frac{C_a - C_i}{C_a}\right) + e_b\left(\frac{C_i}{C_a}\right)$$

Here, e_d and e_b represent the isotopic fractionations associated with the diffusion of CO_2 through the stomata into the leaf (−4.4‰) and the biochemical fixation of CO_2 involving the enzyme Rubisco (−30‰ [104]), respectively. $\delta^{13}C_{atm}$ is the $\delta^{13}C$ value of atmospheric CO_2 (about −8‰ on the VPDB scale) and $\delta^{13}C_{plant}$ represents the $\delta^{13}C$ value of the photosynthate (normally ranging from −22‰ up to −28‰ versus VPDB). The plant regulates evaporation of water from the leaf through the stomata. The same pores are used to acquire CO_2 for photosynthesis. With the stomata fully open (no water stress) net diffusional discrimination against $^{13}CO_2$ becomes negligible, the enzymatic discrimination dominates the isotopic composition of the photosynthate. The limit of the full enzymatic discrimination at $C_i = C_a$ ($\delta^{13}C_{plant} =$ −38‰ versus VPDB) is, however, never achieved. An increase in water pressure deficit at constant leaf temperature is generally associated with a decrease in stomatal conductance and consequent decrease in C_i/C_a [105,106]. Diffusion of CO_2 through the stomata openings now takes full effect and a decrease of $\delta^{13}C_{plant}$ might be expected. However, the negative impact of the discrimination is compensated by far by the fact that the internal CO_2 is utilised to a much larger extend, thereby compensating effectively the full Rubisco discrimination. The limiting case would be a complete uptake of the CO_2 entering through the stomata, with a resulting $\delta^{13}C_{plant}$ of about −12‰. As a consequence, more positive $\delta^{13}C$ values (less overall isotopic discrimination) are predicted when ambient conditions become drier. A high precision measurement of $^{13}C/^{12}C$ in tree rings therefore provides a record of the water pressure deficit during plant growth, which in turn is related to local climate.

Oxygen and hydrogen isotope ratios in atmospheric precipitation correlate with temperature. Hydrogen in organic matter including tree rings derives from water taken up by the roots. The signature of δ^2H (and mostly also $\delta^{18}O$) in rain water is preserved to a large extent in wood cellulose (after some constant isotopic alteration during cellulose formation). By analysing the isotopic composition of cellulose one can infer changes in the isotopic composition of past rainfall. These changes are often linked to relative humidity and to temperature. For a review of water isotopes in plants (mainly hydrogen) see White [107].

A number of studies have utilised the described isotope fractionation effects in plants. As an example, $\delta^{13}C$ and $\delta^{18}O$ measurements on stem cellulose of *Tamarix jordanis* have provided an independent estimate of the relative humidity of an arid region of Israel [108]. This study also showed the possibility of using these parameters to derive the $\delta^{13}C$ of atmospheric CO_2. Stem water $\delta^{18}O$ reflects the mean $\delta^{18}O$ value of source water used by the plant [109]. Variations in $\delta^{18}O$ values of stem cellulose of *T. jordanis* at Masada (Israel) were used by Lipp et al. [103] to normalise the results for cellulose to the same source water signature. Thus, the difference in $\delta^{18}O$ values between leaf cellulose and site specific stem water allows a separation of effects caused by ambient conditions from those associated with isotopic source effects, at least for species specific experiments.

Lipp et al. [103] showed a strong relationship between relative humidity and $\delta^{13}C$ values of stem cellulose. For areas with high moisture supply (RH = 67%) a prominent depletion of $\delta^{13}C$ values (−28‰) was found, whereas in an areas of low moisture supply (RH = 35%) an enrichment (−25‰) was noted for the same species.

Freyer [110] estimated the rate of change in atmospheric $\delta^{13}C$ during 1800–1970 A.D. based on tree ring $\delta^{13}C$ analyses. The value reported was −0.012‰ per year, lower than estimates from other proxies. The record represents a long time period where changes may have been less prominent. The contemporary decrease in $\delta^{13}C$ has accelerated during the last 35 years.

The recent advancement in our understanding of $^{13}C/^{12}C$ discrimination effects during C_3 photosynthesis also has provided a useful tool to estimate long term responses of the photosynthetic mechanism to changing climate and increasing CO_2 concentration. Berninger et al. [111] showed good agreement between actual measurements of tree ring isotopes from Finland and $\delta^{13}C$ estimates, predicted on the basis of the theoretical relationship between discrimination effects of carbon isotopes and the ratio of substomatal to ambient CO_2 concentration. They also observed a long term trend of increasing photosynthetic discrimination ($\delta^{13}C$) of 0.016‰ per year since 1920 in their study.

3.9. Reconstruction of pCO_2 using $\delta^{13}C$ of molecular and total organic carbon from ocean sediments as well as carbonate from terrestrial soil

The history of carbon dioxide concentration in surface oceans and in the atmosphere can be estimated using stable isotope ratio measurements. Two techniques have been established in recent years to estimate the past CO_2 level in ocean and atmosphere: (1) Pagani et al. [112] used the $\delta^{13}C$ composition of alkenones in ancient ocean sediments to derive the pCO_2 level in the surface layer and (2) Cerling [113] introduced a CO_2 paleobarometer utilising $\delta^{13}C$ of pedogenic carbonates in paleosols.

(1) Several studies [114,115] have shown that the overall effect of isotopic fractionation associated with marine photoautotrophic carbon fixation is, in part, proportional to the concentration of available CO_2. This relationship provides a starting point for interpreting isotopic trends of marine sedimentary organic carbon (δ_{TOC}) as a historical $\delta^{13}C$ record for planktonic biomass composition. This has allowed to estimate past surface-water CO_2 concentrations ([116,117] and references therein). Using δ_{TOC} to reconstruct paleo-CO_2 is, however, complicated by several factors. Invariably, δ_{TOC} results from an integration of primary and secondary isotopic signals. More recently compound specific isotopic analysis of molecular markers derived from phytoplankton has been utilised as a more reliable proxy for surface water CO_2 [112]. Organic matter preserved in ocean sediments is comprised of organic compounds some of which are specifically traceable to the organisms that produced them. Such biomarkers are long-chain alkenones in sediment cores. Because these alkenones are largely unaltered through time they can provide information about changes in primary productivity, sea-surface temperature and atmospheric carbon dioxide levels in the past. The quantitative relationship between the availability of dissolved carbon dioxide and isotopic fractionation in some of the planktons has been calibrated experimentally [118]. Estimates of isotopic fractionation in the past can therefore be made from a combined measurement of $\delta^{13}C$ in alkenones and in the calcareous shells of planktonic foraminifera preserved in dated sediment cores. Given such estimates, the dissolved carbon dioxide concentration of surface waters in which the organism grew can be calculated using the calibration relationship.

Isotopic analysis is made using a GC combustion system as described above (Fig. 3). Using this experimental approach, Pagani et al. [119] evaluated specific molecular markers (alkadienones) from organic matter preserved in Miocene ocean sediments from the North and South Atlantic and estimated the pCO_2 level from the $\delta^{13}C$ composition. The results (Fig. 15a) show that pCO_2 steadily increased starting from a low value at 14 Ma (∼180 ppm) and stabilising during the late Miocene at 9 Ma with concentrations between 320 and 250 ppmv. These uniformly low pCO_2 values are consistent with middle to late Miocene alkenone-based pCO_2 estimates and trends from other localities or other types of more indirect proxies (stomatal index, Boron isotopes in foraminifera, etc. [112]).

(2) While it is possible to estimate pCO_2 concentrations of the past from the carbon isotopic composition of ocean sediments, there are few other

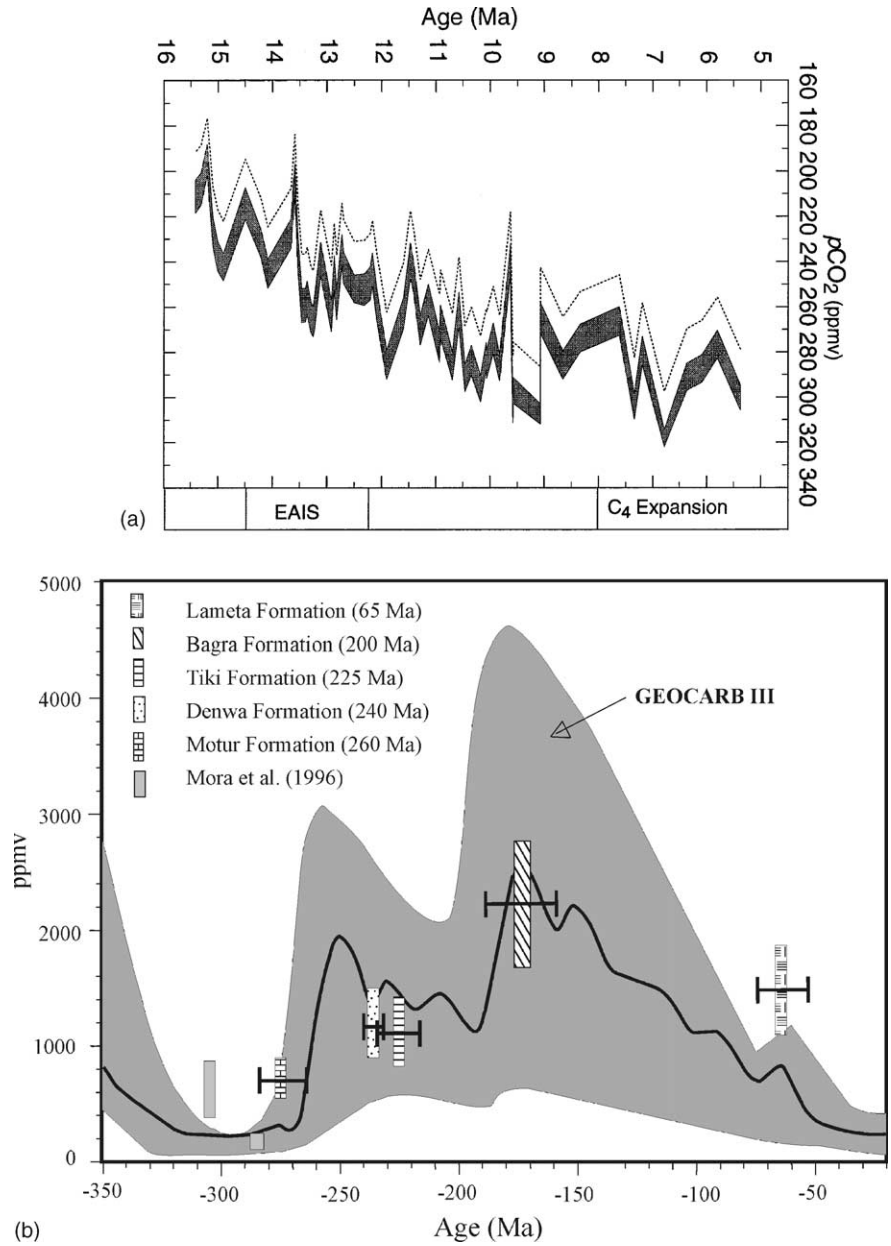

Fig. 15. (a) Maximum pCO_2 estimates calculated on the basis of the carbon isotopic composition of the di-unsaturated alkenones. The record shows an increase in pCO_2 concentration during the Miocene period (reproduced from Pagani et al. [141]). (b) Estimated concentration of atmospheric CO_2 (expressed relative to present-day concentration) as a function of time. The points are based on isotopic analysis of pedogenic carbonates. The dashed curve along with the envelope (error range) is obtained from GEOCARB III (Berner and Kothavala [124]).

pCO_2 proxies in terrestrial ecosystem, which have been used for Phanerozoic pCO_2 reconstruction. Pedogenic carbonates have been proposed as an indirect method to estimate the palaeo-CO_2 concentration in the atmosphere [113,120,121] and palaeosol carbonates are thought to preserve the isotopic composition of local soil CO_2; that primarily reflecting the type of vegetation (e.g., fraction of C_3 versus C_4 plants (see footnote 2)) in the ecosystem [100]. Soil CO_2 may be considered as mainly a mixture of two components: (i) plant and microbially respired CO_2 and (ii) atmospheric CO_2. Mixing of atmospheric CO_2 with respired CO_2 is primarily governed by diffusion. Today, except for ecosystems with very low productivity such as deserts, the atmospheric contribution of total soil CO_2 is small because of the rather low concentration of CO_2 in the modern atmosphere compared to that in the soil air. However, at higher atmospheric CO_2, as has occurred in the distant past, atmospheric CO_2 invasion may have made a significant contribution to total soil CO_2, this resulting in significant isotopic shifts in the $\delta^{13}C$ of soil carbonate precipitated. Therefore, $\delta^{13}C$ analysis of pedogenic carbonates have been taken to provide evidence for large variations in pCO_2 in geologic past [119,122,123]. A knowledge of past carbon dioxide levels and associated paleo-environmental and paleo-ecologic changes are useful for predicting future consequences of the current increase in atmospheric carbon dioxide.

Estimates of CO_2 variations based on equations governing the CO_2 outgassing and weathering reactions are formulated in the GEOCARB II model of Berner [86] and more recently in GEOCARB III [124]. Fig. 15b provides the model simulation of past CO_2 levels. It shows that in the Early Phanerozoic (550 Ma) the pCO_2 was 20 times the present atmospheric level (PAL). Subsequently, pCO_2 declined during the Middle and Late Palaeozoic (450–280 Ma) to reach a minimum (approximately similar to the PAL) at about 300 Ma. The period between 300 and 200 Ma was again characterised by a rapid rise and pCO_2 increased to 5 times the PAL. It was followed by a gradual decline to the PAL with a small peak in the early Tertiary. Such large changes in pCO_2 in the geologic past must have had significant impacts upon climate, biota and surface processes on earth [122]. Therefore, understanding the nature of variation in atmospheric pCO_2 is important for a better understanding of the Earth's physical and biotic history. Ghosh et al. [121] determined the atmospheric CO_2 concentration using Gondwana soil carbonates from India (plotted in Fig. 15b). The mean $\delta^{13}C$ values of the palaeosol carbonates were used to obtain the individual ranges of pCO_2 values presented in the figure. These values represent first independent estimates of atmospheric CO_2 levels during 260–65 Ma bp from soils formed on the (southern hemisphere) Gondwana supercontinent. This is considered an important period in the evolution model as it predicts an increase in the CO_2 level after the early Permian low (310–285 Ma) and ascribes it to an enhanced rate of degassing. The figure shows that a reasonable agreement of the derived CO_2 concentration with Berner's prediction [125] between 275 and 160 Ma has been obtained. However, the abundance of carbondioxide for 65 Ma (Lameta) is 1480 ppm, about twice the value in Berner's mass balance model estimates (560 Ma, GEOCARB III) [124].

4. Climate models and experimental validation

Climate modelling efforts in general aim at a quantitative understanding of the processes driving the Earth's climate system. The complexity of this system requires to create models that incorporate contemporary knowledge and that remain open for new information from future research. In order to validate an individual model it must be able to reproduce experimental observations in space and time.[9]

[9] As an introduction to climate modelling we recommend refs. [3,126,127] for further reading.

The simplest model is represented by a box. The box has source and sink processes for air constituents including chemical reactions and their physicochemical properties, water evaporation and condensation, advective processes, radiation, emission from human sources and so on. The size of the box depends on the problem to be modeled. As an example, the local climate of an urban environment could be modeled by selecting the size of the box slightly larger than the environment itself and parameterise advection from other information. Alternatively, the environment could be modeled using a number of smaller boxes communicating their input/output to each other in order to learn something about the distribution of a specific pollutant originating from one of the boxes within the selected environment over time. The latter approach requires prior knowledge about transport processes between the boxes.

The more complex the environment becomes, the more difficult is quantitative modelling. On the other hand, computing power has increased dramatically in the past and so has our ability to simulate climate using coupled boxes. The whole atmosphere in currently used models is composed of a grid of boxes in all three dimensions with individual properties. In order to calculate the varying contents of the boxes over time and space, the 3D grid is fed with prior information like trace gas concentration and isotope ratio data from sampling stations and remote sensing as input variables constraining the calculations of monthly temporal fluxes. The model output delivers information like temperature, precipitation, etc. The modelling efforts are fine tuned to reproduce the atmospheric trace gas concentration and seasonal signals from new observations at ground stations. Signals at any monitoring station can be modeled providing a world wide spatial coverage with the option to incorporate new stations or to judge where on earth a new station would have the largest scientific benefit. Model precision increases with the number of stations around the globe, with the number of observations on those stations and with the quality of the data.

Modern climate models can be divided into two broad categories: (1) general circulation models (GCM's) and (2) statistical–dynamical models, which include energy balance models (EBM's) and two dimensional zonally averaged dynamic models [124]. Both types of models have been used for modelling palaeoclimatic conditions. GCM's have been used for simulating palaeoclimatic processes like precipitation, temperature, etc. which depend mostly on land/sea distribution, atmospheric flow patterns and distribution as well as concentration of aerosols or trace gases in the global atmosphere [128,129]. Statistical dynamic models have mainly been used for long term climatic simulation experiments [130–132].

Simulation of sudden events and/or prominent features in palaeo-climatic records provides a critical test for GCM's [133]. Evaluation of model results has opened new opportunities for interdisciplinary paleoclimate research and simulated (a) the compilation of data sets that are global in scope and (b) the development of increasingly sophisticated methods for palaeo-environmental analyses. The data sets and analyses are routinely used to check the performance and improve climate models. For example, Kutzbach et al. [134] describe results of climate simulations for 21,000, 16,000, 14,000, 11,000 and 6000 years before present (bp); the output of these simulation experiments were used for biome (vegetation type) reconstruction. The computer experiments were performed using the CCM1 climate model code from NCAR (National Center for Atmospheric Research in Boulder, CO, USA) which features full annual cycle simulation, linked with land surface modelling and a mixed layer ocean structure. Introduction of these features results in a global mean temperature change at the Last Glacial Maximum (LGM, 18 ka bp) of $-6.5\,^{\circ}C$ compared to today. Overall, the LGM was found to be cooler and drier similar to actual observations discussed before. Felzer et al. [135] used NCAR CCM1 to isolate the individual effects of orbital forcing, ice sheet size and lower CO_2 concentration on climate during and since the LGM. Their study shows that surface temperatures both globally and regionally are linear functions of the individual response to ice sheets, CO_2 concentrations and insolation. At the LGM, the global mean temperature decrease of

−6.5 °C is about half that from the ice sheet alone. The other half originates from the lower CO_2 concentration. However, at 11 ka bp the response is mainly due to orbitally forced changes in insolation.

Whereas these results were generated by conventional climate modelling which must also simulate temperature and precipitation from experimental proxies, new approaches are explicitely based on first principles. Hoffmann et al. [136] modified the ECHAM GCM by including the water isotopes (D/H and $^{18}O/^{16}O$) from first principles and were thus able to simulate the distribution and variability of these isotope ratios in great detail and compare the model output directly with the measured isotope values from Greenland and Vostok.

The analyses of cores from ice sheets in the Antarctic and Greenland as well as cores from the sea- and lake-floors suggest that the global average temperature was more than 5 °C lower compared with the current value [68] during LGM. Prentice et al. [137] used the pollen and lake level data set and biomisation techniques to estimate climatic parameters during 6 ka and compared them with model simulations using CCM1. The data estimates agree with the model simulations in that the growing seasons were warmer in northern and central Europe at 6 ka than they are today and the warmer winters at 6 ka prevented boreal conifers from spreading westwards in central and eastern Europe. However, the simulation experiment failed to demonstrate the observation that around 6 ka bp the climate over northern Africa was wetter than today and that the Sahara desert was green as suggested from Biome reconstruction of North Africa [138,139]. Further modelling efforts are necessary to fully quantify the contributions of different feed back mechanisms in order to narrow the gaps between model output and actual observations.

5. Summary and conclusion

In this review we have attempted to summarise how our understanding of global climatic change has been advanced by making use of high precision stable isotope analyses. Significant progress was made owing to new developments in sample preparation and mass spectrometric measurement techniques capable to distinguish small signals or variations in isotopic composition in samples of air, water and ocean or terrestrial sediments collected from different geographical provinces. Our understanding of the variability in global climate at present is based on direct human observation on nature and extended into the past by indirect means with careful retrieval of preserved information from natural archives denoting long term variation of global climate.

Key components of using stable isotope information in climate change are:

- isotope-tailored mass spectrometry and dedicated extraction systems for analysis of individual components, so that signals of climate variability from natural sources including air can be recovered.
- natural archives, providing information about how different components of the environment are coupled and have interacted in the past. Historical records of air composition and temperature change are available for the last two centennia at most, mainly based on direct observation. Some of this information can be recovered and further extended into the past from archeological documents. Air inclusions in firn and ice provide an important natural archive for reconstructing historical trace gas concentrations as well as isotope records. Tree rings can be used to retrieve climatic information for the last 10,000 years whereas water in ice cores can go back in time up to 400,000 years. Sedimentary deposits and corals provide an indirect approach to the past, mainly to understand the climate evolution on a geological time scale. The isotopic signature from such archives is often difficult to extract and requires considerable experience. As an example, oxygen isotopes from carbonates must be measured from selected species (foraminifera) that have a broad coverage in time and that have remained constant in their physiology. Most importantly the fossils must have remained immune against isotopic fractionation over time.

- development of a thorough theoretical understanding of the climate system as a whole on the basis of validated experimental observations using global climate model simulations. The global synthesis of palaeo-climate data combined with analyses of palaeo-climatic simulations provides a mathematical handle to future consequences of contemporary climate change.

Major future challenges are to improve inter-laboratory precision of isotopic measurements in order to compare results from different laboratories on a very high level of precision. In addition, the isotopic connection of different chemical species or different types of archives needs further improvement, and the (isotopic) fractionation between compartments is not established well enough to allow conclusions to be drawn unequivocally. Models require experimental input of roughly equivalent quality and a high spatial density which is difficult to get for the present and impossible to provide for the past. For reducing the uncertainty of our understanding of the Earth's climate system, the puzzle needs more pieces.

Acknowledgements

We are grateful to Martin Heimann, Jon Lloyd, Roland A. Werner and Philipp Hoelzmann, all from the Max Planck Institute for Biogeochemistry in Jena, for helpful discussions and critical suggestions. We also appreciate the comments of two anonymous reviewers which helped to improve the manuscript.

References

[1] A. Berger, Rev. Geophys. 26 (1988) 624.
[2] J. Imbrie, J.Z. Imbrie, Science 207 (1980) 943.
[3] T.E. Graedel, P.J. Crutzen, Atmosphic Change: An Earth System Perspective, W.H. Freeman and Company, New York, Oxford, 1993, ISSN 0-7167-2334-4.
[4] G. Marland, T. Boden, R.J. Andres, Id_járás 99 (1995) 157; G. Marland, B. Schladminger, Energy 20 (1995) 1131; R.J. Andres, D.J. Fielding, G. Marland, T.A. Boden, N. Kumar, A.T. Kearney, Tellus B 51 (1999) 759.
[5] R.T. Watson, I.R. Noble, Challenges of a Changing Earth, Springer-Verlag, New York, IGBP Series, 2002.
[6] Intergovernmental Panel for Climate Change (IPCC), Third Assessment Report—Climate Change 2001, http://www.ipcc.ch/.
[7] C.D. Keeling, Geochim. Cosmochim. Acta 24 (1961) 277.
[8] C.D. Keeling, T.P. Whorf, M. Wahlen, J. van der Plicht, Nature 375 (1995) 666.
[9] H. Craig, Geochim. Cosmochim. Acta 12 (1957) 133.
[10] T.B. Coplen, C. Kendall, J. Hopple, Nature 302 (1983) 236.
[11] T.B. Coplen, Nature 375 (1995) 285; T.B. Coplen, Pure Appl. Chem. 66 (1994) 273.
[12] E.T. Sundquist, Science 259 (1993) 934.
[13] M. Scholze, W. Knorr, M. Heimann, HOLOCENE 13 (2003) 327.
[14] G.D. Farquhar, M.H. O'Leary, J.A. Berry, Aust. J. Plant Physiol. 9 (1982) 121.
[15] J. Lloyd, G.D. Farquhar, Oecologia 99 (1994) 201.
[16] P.P. Tan, in: B. Bolin (Ed.), Carbon Cycle Modelling, SCOPE 16, Wiley, Chichester, 1981.
[17] W.G. Mook, J.C. Bommerson, W.H. Staverman, Earth Planet. Sci. Lett. 22 (1974) 169.
[18] R. Francois, M. Altabet, R. Goericke, D. McCorkie, C. Brunet, A. Poisson, Global Biogeochem. Cycl. 7 (1974) 627.
[19] G.I. Pearman, P. Hyson, J. Atoms. Chem. 4 (1986) 81.
[20] C.D. Keeling, R.B. Bacastow, A.F. Carter, S.C. Piper, T.P. Whorf, M. Heimann, W.G. Mook, H. Roeloffzen, in: D.H. Peterson (Ed.), Geophysical Monograph Series 55, AGU, Washington, DC, 1989.
[21] M. Heimann, E. Maier-Reimer, Global Biogeochem. Cycl. 10 (1996) 89.
[22] R.J. Francey, P.P. Tans, Nature 327 (1987) 495.
[23] G.D. Farquhar, J. Lloyd, J.A. Taylor, L.B. Flanagan, J.P. Syvertsen, K.T. Hubick, C.S. Wong, J.R. Ehleringer, Nature 363 (1993) 439.
[24] S.B. Jacobsen, F. Fong, R. Heath, Plant Physiol. 55 (1975) 468.
[25] M. Cuntz, P. Ciais, G. Hoffmann, Tellus B 54 (2002) 895.
[26] G.B. Allison, J.R. Gat, F.W.J. Leaney, Chem. Ecol. (Isot. Geosci. Sec.) 58 (1985) 145.
[27] D. Yakir, in: H. Griffith (Ed.), Stable Isotopes, Integration of Biological and Geochemical Processes, BIOS Scientific Publishers, Oxford, 1998, p. 147, ISBN 1859961355.
[28] K. Rozanski, A.L. Araguas, R. Gonfiantini, Geophysical Monograph Series (IUGG), 1993.
[29] B.F. Murphy, Phys. Rev. 72 (1947) 834.
[30] www.iaea.org/programmes/rial/pci/isotopehydrology
[31] C.E. Allison, R.J. Francey, H.A.J. Meijer, IAEA-TECDOC 825 (1995) 155.
[32] J. Bigeleisen, M.J. Perlman, H. Prosser, Anal. Chem. 24 (1952) 1356.
[33] D.A. Merritt, J.M. Hayes, Anal. Chem. 66 (1994) 2336.
[34] D.F. Ferretti, D.C. Lowe, R.J. Martin, G.W. Brailsford, J. Geophy. Res. Atmos. 105 (2000) 6709.
[35] J. Koziet, J. Mass Spectrom. 32 (1997) 103.
[36] B.E. Kornexl, M. Gehre, R. Hoefling, R.A. Werner, Rapid Commun. Mass Spectrom. 13 (1999) 1685.
[37] A.W. Hilkert, C.B. Douthitt, H.J. Schlüter, W.A. Brand, Rapid Commun. Mass Spectrom. 13 (1999) 1226.

[38] S. Epstein, T. Mayeda, Geochim. Cosmochim. Acta 4 (1953) 213.
[39] M. Leuenberger, C. Huber, Anal. Chem. 74 (2002) 4611.
[40] R.F. Francey, H.S. Goodman, in: R.J. Francey, B.W. Forgan (Eds.), Baseline Atmospheric Program 1983–1984, Division of Atmospheric Research, CSIRO, Australia, 1985.
[41] C.E. Allison, R.J. Francey, in: J.L. Gras, N. Derek, N.W. Tindale, A.L. Dick (Eds.), Baseline Atmospheric Program 1996, Division of Atmospheric Research, CSIRO Australia, 1999, p. 44.
[42] J.W.C. White, D.F. Ferretti, B.H. Vaughn, R.J. Francey, C.E. Allison, IAEA-TECDOC 1268 (2002) 3.
[43] M. Trolier, J.W.C. White, P.P. Tans, K.A. Masarie, P.A. Gemery, J. Geophys. Res. 101 (1996) 25897.
[44] P. Ciais, P.P. Tans, M. Trolier, J.W.C. White, R.J. Francey, Science 269 (1995) 1098.
[45] R.A. Werner, M. Rothe, W.A. Brand, Rapid Commun. Mass Spectrom. 15 (2001) 2152.
[46] W.A. Brand, J. Mass Spectrom. 31 (1996) 225.
[47] W.G. Mook, S. van der Hoek, Isot. Geosci. 1 (1983) 237.
[48] C.E. Allison, R.J. Francey, L.P. Steele, IAEA-TECDOC 1269 (2002) 5.
[49] E. Moor, B.J. Stauffer, J. Glaciol. 30 (1984) 358.
[50] H. Friedli, H. Lötscher, H. Oeschger, U. Siegenthaler, B. Stauffer, Nature 324 (1986) 237.
[51] M.C. Leuenberger, M. Eyer, P. Nyfeler, B. Stauffer, T.F. Stocker, Tellus B 55 (2003) 138.
[52] W.A. Brand, Isot. Environ. Health Stud. 31 (1995) 277.
[53] J.M. McCrea, J. Chem. Phys. 18 (1950) 849.
[54] N.J. Shackleton, N.D. Opdyke, Quat. Res. 3 (1973) 39.
[55] R.K. Mathews, W.B. Curry, K.C. Lohman, M.A. Sommer, R.Z. Poore, Nature 283 (1980) 555.
[56] P.K. Swart, S.J. Burns, J.J. Leder, Chem. Geol. (Isot. Geosci. Sec.) 86 (1991) 89.
[57] R.J. Francey, C.E. Allison, D.M. Etheridge, I.G. Trudinger, M. Enting, M. Leuenberger, R.L. Langenfelds, E. Michel, L.P. Steele, Tellus B 51 (1999) 170.
[58] P.J. Rayner, I.G. Enting, R.J. Francey, R. Langenfelds, Tellus B 51 (1999) 213.
[59] P. Ciais, A.S. Denning, P.P. Tan, J.A. Berry, D.A. Randall, G.J. Collatz, P.J. Sellers, J.W.C. White, M. Trolier, H.A.J. Meijer, R.J. Francey, P. Monfray, M. Heimann, J. Geophys. Res. 102 (1997) 5857.
[60] P. Peylin, P. Ciais, A.S. Denning, P.P. Tans, J.A. Berry, J.W.C. White, Tellus B 51B (1999) 642.
[61] P. Ciais, H.A.J. Meijer, in: H. Griffith (Ed.), Stable Isotopes, Integration of Biological and Geochemical Processes, BIOS Scientific Publishers, Oxford, 1998, p. 409, ISBN 1859961355.
[62] K.A. Masarie, R.L. Langenfelds, C.E. Allison, T.J. Conway, E.J. Dlugokencky, R.J. Francey, P.C. Novelli, L.P. Steele, P.P. Tans, B. Vaughn, J.W.C. White, J. Geophys. Res. 106 (2001) 20445.
[63] D.M. Etheridge, L.P. Steele, R.L. Langenfelds, R.J. Francey, J.M. Barnola, V.I. Morgan, J. Geophys. Res. 103 (1996) 15979.
[64] J.R. Petit, J. Jouzel, D. Raynaud, N.I. Barkov, J.M. Barnola, I. Basile, M. Bender, J. Chappellaz, M. Davis, G. Delaygue, M. Delmotte, V.M. Kotlyakov, M. Legrand, V.Y. Lipenkov, C. Lorius, L. Pepin, C. Ritz, E. Saltzman, M. Stievenard, Nature 399 (1999) 429.
[65] D. Wagenbach, Environmental Records in Alpine Glaciers and Ice Sheets. Dahlem Konferenzen, Wiley, Chichester, 1989, p. 69.
[66] W. Dansgaard, J.W.C. White, S.J. Johnsen, Nature 339 (1989) 532.
[67] S.J. Johnsen, H.B. Clausen, W. Dansgaard, N.S. Gundestrup, C.U. Hammer, U. Andersen, K.K. Andersen, C.S. Hvidberg, D. Dahl-Jensen, J.P. Steffensen, H. Shoji, A.E. Sveinbjornsdottir, J. White, J. Jouzel, D. Fisher, J. Geophys. Res. Oceans 102 (1997) 26397.
[68] C. Lorius, J. Jouzel, C. Ritz, L. Merlivat, N.I. Barbov, Y.S. Korotkevich, V.M. Kotlyakov, Nature 316 (1985) 591.
[69] J. Jouzel, C. Waelbroeck, B. Malaize, M. Bender, J.R. Petit, M. Stievenard, N.I. Barkov, J.M. Barnola, T. King, V.M. Kotlyakov, V. Lipenkov, C. Lorius, D. Raynaud, C. Ritz, T. Sowers, Clim. Dyn. 12 (1996) 513.
[70] H. Craig, Science 133 (1965) 1702.
[71] M.K. Gagan, L.K. Ayliffe, J.W. Beck, J.E. Cole, E.R.M. Druffel, R.B. Dunbar, D.P. Schrag, Quat. Sci. Rev. 19 (2000) 45.
[72] J. Zachos, M. Pagani, L. Sloan, E. Thomas, K. Billups, Science 292 (2001) 686.
[73] W.A. Berggren, D.V. Kent, C.C.I. Swisher, M.P. Aubry, Soc. Sediment. Geol. 54 (1995) 129.
[74] P.A. Scholle, M.A. Arthur, Am. Assoc. Petrol. Geol. Bull. 64 (1980) 67.
[75] J. Veizer, W.T. Holser, C.K. Wilgus, Geochim. Cosmochim. Acta 44 (1980) 579.
[76] M.A. Arthur, W.E. Dean, S.O. Schlanger, Geophys. Monogr. 32 (1985) 504.
[77] N.J. Shackleton, Geophys. Monogr. 32 (1985) 412.
[78] J.L. Banner, Sedimentology 42 (1995) 805.
[79] J.L. Banner, G.N. Hanson, Geochim. Cosmochim. Acta 54 (1990) 3123.
[80] A.H. Knoll, J.M. Hayes, A.J. Kaufman, K. Swett, L.B. Lambert, Nature 321 (1986) 832.
[81] L.A. Derry, A.J. Kaufman, S.B. Jacobsen, Geochim. Cosmochim. Acta 56 (1992) 1317.
[82] P.M. Kroopnick, Deep Sea Res. 3 (1985) 57.
[83] T.A. McConnaughey, J. Whelan, Earth Sci. Rev. 42 (1997) 95.
[84] A.J. Kaufman, A.H. Knoll, S.M. Awramik, Geology 20 (1992) 181.
[85] R.A. Berner, A.C. Lasaga, R.M. Garrels, Am. J. Sci. 283 (1983) 641.
[86] R.A. Berner, Am. J. Sci. 294 (1994) 56.
[87] J. Veizer, D. Ala, K. Azmy, P. Bruckschen, D. Buhl, F. Bruhn, G.A.F. Carden, A. Diener, S. Ebneth, Y. Godderis, T. Jasper, G. Korte, F. Pawellek, O.G. Podlaha, H. Strauss, Chem. Geol. 161 (1999) 59.
[88] M.T. McCulloch, M.K. Gagan, G.E. Mortimer, A.R. Chivas, P.J. Isdale, Geochim. Cosmochim. Acta 58 (1994) 2747.

[89] H. Craig, L. Gordon, in: E. Tongiorgio (Ed.), Stable Isotopes in Oceanographic Studies and Paleotemperatures, Consiglio Nazionale delle Richerche, Pisa, 1965, p. 9.
[90] G. Faure, Principles of Isotope Geology, 2nd ed. Wiley, New York.
[91] M.K. Gagan, A.R. Chivas, Geophys. Res. Lett 22 (9) (1995) 1069.
[92] R.G. Fairbanks, M.N. Evans, J.L. Rubenstone, R.A. Mortlock, K. Broad, M.D. Moore, C.D. Charles, Coral Reefs 16 (1997) S93.
[93] C.H. Hendy, Geochim. Cosmochim. Acta 35 (1971) 801.
[94] R.S. Harmon, S.P. Thompson, H.P. Schwarcz, D.C. Ford, Natl. Speleol. Soc. Bull. 37 (1975) 21.
[95] T.C. Atkinson, R.S. Harmon, P.L. Smart, A.C. Waltham, Nature 272 (1978) 24.
[96] A. Goede, R.S. Harmon, J. Geol. Soc. Aust. 30 (1983) 89.
[97] L.K. Ayliffe, H.H. Veeh, Chem. Geol. 72 (1989) 211.
[98] G.A. Brook, D.A. Burney, B.J. Cowart, Palaeo. Palaeo. Palaeo. 76 (1990) 311.
[99] J.A.DoraleJ.A. Dorale, L.A. Gonzalez, M.K. Reagen, D.A. Pickett, M.T. Murrell, R.G. Baker, Science 258 (1992) 1626.
[100] M. Baskaran, R.V. Krishnamurthy, Geophys. Res. Lett. 20 (1993) 2905.
[101] T.E. Cerling, Earth Planet. Sci. Lett. 71 (1984) 229.
[102] G.D. Farquhar, M.H. O'Leary, J.A. Berry, Aust. J. Plant Physiol. 9 (1982) 121.
[103] J. Lipp, P. Trimborn, T. Edwards, Y. Waisel, D. Yakir, Geochim. Cosmochim. Acta 60 (1996) 3305.
[104] M. O'Leary, in: J.R. Ehleringer, A.E. Hall, G.D. Farquhar (Eds.), Stable Isotopes and Plant Carbon–Water Relations, Academic Press, San Diego, CA, 1993, p. 19.
[105] P.J. Aphalo, P.G. Jarvis, Plant Cell Environ. 14 (1991) 127.
[106] K.A. Mott, D.F. Parkhurst, Plant Cell Environ. 14 (1991) 509.
[107] J.W.C. White, in: P.W. Rundel, J.R. Ehleringer, K.A. Nagy (Eds.), Stable Isotopes in Ecological Research, Springer-Verlag, New York, 1989, p. 143.
[108] D. Yakir, J. Gat, A. Issar, E. Adar, P. Trimborn, J. Lipp, Geochim. Cosmochim. Acta 58 (1994) 3535.
[109] J.R. Ehleringer, T.E. Dawson, Plant Cell Environ. 15 (1992) 1073.
[110] H.D. Freyer, in: J.R. Trabalka, D.E. Reichle (Eds.), Changing Carbon Cycles: A Global Analysis, Springer-Verlag, New York, 1986, p. 125.
[111] F. Berninger, E. Sonninen, T. Aalto, J. Lloyd, Global Biogeochem. Cycl. 14 (2000) 213.
[112] M. Pagani, K.H. Freeman, M.A. Arthur, Geochim. Cosmochim. Acta 64 (2000) 37.
[113] T.E. Cerling, Am. J. Sci. 291 (1991) 377.
[114] G.H. Rau, T. Takahashi, D.J. Des Marais, Nature 341 (1989) 516;
G.H. Rau, T. Takahashi, D.J. Des Marais, D.J. Repeta, J.H. Martin, Geochim. Cosmochim. Acta 56 (1992) 1413.
[115] K.R. Hinga, M.A. Arthur, M.E.Q. Pilson, D. Whitaker, Global Biogeochem. Cycl. 8 (1994) 91.
[116] G.H. Rau, P.N. Froelich, T. Takahashi, D.J. Des Marais, Palaeoceanography 6 (1991) 335.
[117] M.E. Raymo, M. Horowitz, Geophys. Res. Lett. 23 (1996) 367.
[118] R.R. Bidigare, A. Fluegge, K.H. Freeman, K.L. Hanson, J.M. Hayes, D. Hollander, J.P. Jasper, L.L. King, E.A. Laws, J. Milder, F.J. Millero, R. Pancost, B.N. Popp, P.A. Steinberg, S.G. Wakeham, Global Biogeochem. Cycl. 11 (1997) 279.
[119] M. Pagani, M.A. Arthur, K.H. Freeman, Palaeoceanography 14 (1999) 273.
[120] D.D. Ekart, T.E. Cerling, I.P. Montanez, N.J. Tabor, Am. J. Sci. 299 (1999) 805.
[121] P. Ghosh, P. Ghosh, S.K. Bhattacharya, Palaeo. Palaeo. Palaeo. 170 (2001) 219.
[122] P. Ghosh, S.K. Bhattacharya, R.A. Jani, Palaeo. Palaeo. Palaeo. 114 (1995) 285.
[123] C.I. Mora, S.G. Driese, L.A. Colarusso, Science 271 (1996) 1105.
[124] R.A. Berner, Z. Kothavala, Am. J. Sci. 301 (2001) 182.
[125] J.E. Kutzbach, Adv. Geophys. 28A (1985) 159.
[126] T.E. Graedel, P.J. Crutzen, Atmosphere, Climate and Change, Scientific American Library, New York, 1997, ISSN 0-7167-6028-2.
[127] H.V. Storch, S. Güss, M. Heimann, Das Klimasystem und seine Modellierung—eine Einführung, Springer-Verlag, Heidelberg, 1999, ISBN 3-540-65830-0 (in German).
[128] W.L. Prell, J.E. Kutzbach, J. Geophys. Res. 92 (1987) 8411.
[129] D. Rind, D. Peteet, G. Kukla, J. Geophys. Res. 94 (1989) 12851.
[130] A. Berger, H. Gallee, T. Fichefet, I. Marsiat, C. Tricot, Palaeo. Palaeo. Palaeo. 89 (1990) 125.
[131] G. Deblonde, W.R. Peltier, J. Geophys. Res. 96 (1991) 9189.
[132] H. Gallee, J.P. van Ypersele, T. Fichefet, I. Marsiat, C. Tricot, A. Berger, J. Geophys. Res. 97 (1992) 15713.
[133] T. Webb, J.E. Kutzbach, Quat. Sci. Rev. 17 (1998) 465.
[134] J.E. Kutzbach, R. Gallimore, S.P. Harrison, P. Behling, R. Selin, F. Laarif, Quat. Sci. Rev. 17 (1998) 473.
[135] B. Felzer, T. Webb, R.J. Oglseby, Quat. Sci. Rev. 17 (1998) 507.
[136] G. Hoffmann, M. Werner, M. Heimann, J. Geophys. Res. Atmos. 103 (1998) 16871.
[137] I.C. Prentice, S.P. Harrison, D. Jolly, J. Guiot, Quat. Sci. Rev. 17 (1997) 659.
[138] S.P. Harrison, D. Jolly, F. Laarif, A. Abe-Ouchi, B. Dong, K. Herterich, C. Hewitt, S. Joussaume, J.E. Kutzbach, J. Mitchell, N. De Noblet, P.J. Valdes, Climatology 11 (1998) 2721.
[139] I.C. Prentice, T. Webb III, J. Biogeogr. 25 (1998) 997.
[140] D. Yakir, S.L. da Sternberg, Oecologia 123 (2000) 297.
[141] M. Pagani, K.H. Freeman, M.A. Arthur, Science 285 (1999) 876.